Investigation of Temperature Gradients in a Demonstration Model Thermoacoustic Refrigerator

by:

Steven P. Stoll
In Partial Fulfillment of Departmental Honors Requirements

University of Central Arkansas
Conway, AR 72035
Spring 2008

Thesis Committee:

Advisor:

_____
Dr. William V. Slaton, Ph. D.
Associate Professor of Physics and Astronomy

Reader:

_____
Dr. Carl Frederickson, Ph. D.
Associate Professor of Physics and Astronomy

**Department
Chair:**

_____
Dr. Stephen R. Addison, Ph. D.
Professor and Chair, Department of Physics and Astronomy

Abstract

While using a thermoacoustic system for refrigeration is not as efficient as using vapor compression, it has the advantage of fewer mechanical parts that can fail which makes it more reliable. It is this reliability which warrants further exploration of using the energy of acoustic waves to produce a cooling effect. This project will explore thermoacoustic refrigeration using relatively inexpensive materials. Using air as the operating gas, the goal of this project is to evaluate the effect of stack placement on temperature gradient.

Contents

Basics

From the basic physics of periodic sound waves[5], we get the equation for displacement $s = s_{max} \sin(kx - \omega t)$ and pressure $\Delta P = \Delta P_{max} \cos(kx - \omega t)$. From this, we can see that displacement and pressure are ninety degrees out of phase (see figure D.1). What is not so obvious, is that there is also a temperature oscillation occuring along with the pressure wave[10]. Sound is an adiabatic process, which means that as a volume of gas undergoes displacement, the process occurs without heat transfer into or out of the gas. Schroeder[4] shows that $V^\gamma P$ is constant, where γ is the ratio of specific heats, which is always greater than one. Rearranging the ideal gas law, $PV = NkT$, for V and substituting it back into the previous equation, then rearranging and consolidating the constants, we get $T = P^{\frac{\gamma-1}{\gamma}} C$. From this, we can see that the temperature fluctuates with changes in pressure. [1] It is by using these oscillations that thermoacoustic systems operate.

Consider a small parcel of gas in proximity to a surface, oscillating back and forth over a small region. The pressure of the gas drops as it moves toward the pressure node, the temperature also drops. The gas is now cooler than the nearby surface, so a small amount of heat flows into it (see figure D.2(a)). The parcel then moves toward the pressure anti-node, increasing pressure and temperature. It is now hotter than the nearby surface, so a small amount of heat flows out of it (see figure D.2(b)). Each parcel of gas along the length of the surface acts, in conjuction with the neighboring parcels, to move heat from one end of the surface (near the pressure node) to the opposite end (near the pressure anti-node).

If the parcel of gas is located at the pressure node, it will not undergo pressure changes, and therefore will not absorb or relinquish heat. Conversely, if it is at a velocity node, it will not change position, so all the thermal transfer occurs at the same location. It is only where the gas parcel experiences both velocity and pressure changes that heat pumping along the surface will occur.

Coefficient of Performance

From the first law of thermodynamics, also known as conservation of energy, we get $Q_H = Q_C + W$ (see figure D.3), where W is work done on the system and Q is heat moved with the subscripts H and C for the hot and cold reservoirs. This equation can be rearranged as

$$W = Q_H - Q_C. \tag{1}$$

From the second law of thermodynamics, we get that the entropy of a system must always remain the same or increase, or $\Delta S \geqslant 0$. In an ideal engine or a refrigerator, $\Delta S_{total} = \Delta S_H + \Delta S_C \geqslant 0$, which means the only entropy generated is a result of the heat transfer. For a quasistatic process, as in a thermoacoustic refrigerator, the change in entropy is related to the heat and temperature by

$$\Delta S = \frac{Q}{T}. \tag{2}$$

When (2) is substituted back into $\Delta S_{total} = \Delta S_H + \Delta S_C \geqslant 0$, gives us

$$\frac{Q_H}{T_0} - \frac{Q_C}{T_L} \geqslant 0. \tag{3}$$

---

[1]From Swift's[6] Equation (14) we see that $\frac{T_{AC}}{T_0} = \frac{\gamma-1}{\gamma} \frac{P_{AC}}{P_0}$, which calculated from later data is $\frac{T_{AC}}{T_0} = \frac{1.4-1}{1.4} \frac{4.445\ kPa}{101\ kPa} = 0.0126$. This means the temperature of the air is fluctuating at 1.26% of room temperature.

Which can be rewritten as

$$\frac{Q_H}{T_0} \geqslant \frac{Q_C}{T_L} \quad \text{or} \quad \frac{Q_H}{Q_C} \geqslant \frac{T_0}{T_L}, \tag{4}$$

where T_0 is the temperature of the hot reservoir, and T_L is the temperature of the cold reservoir. Calculation of $\text{COP}_{\text{carnot}}$[4] is a basic cost-benefit calculation, where the benefit is the heat (Q_C) removed from the cold reservoir and the cost is the work required to accomplish it.

$$\text{COP}_{\text{carnot}} = \frac{\text{benefit}}{\text{cost}} = \frac{Q_C}{W} = \frac{Q_C}{Q_H - Q_C} = \frac{Q_C}{Q_C \left(\frac{Q_H}{Q_C} - 1\right)} = \frac{1}{\frac{Q_H}{Q_C} - 1} \tag{5}$$

A refrigerator operating with Carnot's efficiency has the assumption that no new entropy is created. Based on that assumtion, the ratio of heats and temperatures is the same (see equation G.8). We substitute $Q_H/Q_C = T_0/T_L$ into the equation (5) to get the value for $\text{COP}_{\text{carnot}}$.

$$\text{COP}_{\text{carnot}} = \frac{1}{\frac{T_0}{T_L} - 1} = \frac{T_L}{T_0 - T_L} \tag{6}$$

For any real refrigerator, there is always some amount of heat conducted from the region of higher temperature to the lower temperature region. For the thermoacoustic refrigerator, this leakage (Q_i) is determined by the solid area of the stack, the thermal conductivity (κ) of the stack material, the temperature difference (ΔT) and the length of the stack by the relationship:

$$Q_i = A_{stack} \kappa \frac{\Delta T}{L_{stack}} = (1 - \Omega) A_{pipe} \kappa \frac{T_0 - T_L}{L_{stack}} \tag{7}$$

Where Ω is the porosity of the stack. Once this thermoacoustic refrigerator reaches equilibrium the only heat being moved is the amount of heat being conducted by the stack material,

$$Q_H = Q_i + W \quad \text{or} \quad W = Q_H - Qi \tag{8}$$

So the coefficient of performance for this refrigerator is:

$$\text{COP} = \frac{\text{benefit}}{\text{cost}} = \frac{Q_i}{W_{driver}} \tag{9}$$

We can now calculate the coefficient of performance relative to Carnot:

$$\text{COPR} = \frac{\text{COP}}{\text{COP}_{\text{carnot}}} = \frac{Q_i/W_{driver}}{T_L/(T_0 - T_L)} \tag{10}$$

Standing Waves in Pipes

In an open-closed pipe, the closed end of the pipe is a velocity node (zero velocity) because the air molecules are prevented from passing out of the end. Since pressure and velocity are out of phase by ninety degrees, this means the end is a pressure anti-node (maximum pressure). Because only odd harmonics are allowed, and we are interested in only the fundamental frequency,

$$f_0 = c/4L, \tag{11}$$

where c is the speed of sound in air (347.21 m/s).

During the acoustic cycle, the distance over which heat can be conducted through the gas is known as the thermal penetration depth (δ_κ). The thermal penetration depth is determined by the duration of the cycle, which is dependent on frequency (f), and properties of the working gas, such as its thermal conductivity (κ), density (ρ) and isobaric heat capacity (c_p). The equation[10] defining the relationship of these factors to the penetration depth is

$$\delta_\kappa = \sqrt{\frac{\kappa}{\pi f \rho c_p}}. \tag{12}$$

For air at standard temperature and pressure, these values are $\kappa = 0.02624$ W/(m K), $\rho = 1.173$ kg/m^3 and $c_p = 1005$ J/(kg K).

Refrigerator Construction

The refrigerator is built from a driver box, a resonator connector and a resonator section. A pre-existing driver box was used, which is composed of a hollow, clear plastic 30-centimeter diameter cylinder with clear plastic plates bolted to the open ends of the cylinder. The upper plate has a ten-inch speaker mounted on the interior side of it, with a four inch-diameter hole cut into it directly above the center of the speaker. The bottom plate has connectors that allow the speaker to be connected to an outside source. The resonator connector is composed of a disk of plastic with a hole in the center of it, into which a section of glass pipe was epoxied. The connector is bolted onto the upper plate of the driver box, aligned above the hole in the plate. This connector allows different resonators to be attached via standard couplers.

For the straight section of glass pipe there were two different endcaps utilized to seal off one end of the tube, making it act as an open-closed resonator. The first endcap was a pre-existing aluminum disk, into which a microphone could be placed for recording the pressure at the end of the tube. The second endcap had to be fabricated (see figure D.5) in order to permit the use of a heat exchanger and a microphone tube that would allow the pressure to be measured at various points inside the tube. This second endcap is constructed from two disks of plastic that bolt together and have openings through which the microphone tube and the tubes for the heat exchanger pass. Sandwiched between the two layers of plastic are o-rings which allow the various tubes to be moved while still allowing the system to be sealed against pressure loss.

Two stacks were constructed of plastic cocktail straws. One cut to an average length of 5.23 cm and the other cut to an average length of 2.54 cm. The straws are held together with double-sided adhesive tape. The plastic from which the straws are made of is polypropylene, which can have thermal conductivity (κ) values ranging from 0.1 W/(m K) to 0.22 W/(m K).

The porosity (Ω) of the stack is the ratio of open area to the total area of the stack (see figure D.6). The stack is 47.4 mm in diameter, giving a total area of 1576.3 mm^2. Each of the straws that make up the stack has an internal diameter of 2.85 mm, giving it an open area of 6.38 mm^2. The stack is composed of 153 straws, yielding a total open area of 874.06 mm^2. This results in an Ω of 0.619.

In order to prevent the build up of heat in the refrigerator, it was necessary to construct a heat exchanger system. The heat exchanger is made of copper tubing with an outer diameter of 3.17 mm. The central section of the tubing is bent into a circular shape, 50 mm in diameter, at a right angle to the remainder of the tubing (see figure D.7). A circular piece of copper screen mesh whose

wires are 1.3 mm apart, also 50 mm in diameter, is soldered to the circular portion of the copper tubing. In addition to the heat exchanger itself, the system consists of a small pump, submerged in a bucket of water, which is connected to the heat exchanger by plastic tubing. Because the water in the bucket is recycled, the heat being removed from the refrigerator builds up in the water. This necessitated the periodic addition of ice to the bucket to maintain a constant temperature. Later in the project, a Thermo Scientific NESLAB RTE7 refrigerated bath became available to control the temperature of the recycling fluid.

The stack and the heat exchanger are held in contact with each other by use of several copper wires. These copper wires, each of which which extends down through the copper mesh and a pore in the stack, around a toothpick, then back up through another pore and the copper mesh, are pulled and twisted so that the upper surface of the stack maintains tight contact with the lower side of the heat exchanger.

In order to measure the pressure at locations other than the end of the resonance tube, it was necessary to construct a microphone tube. The microphone tube consists of a 30.5 cm straight brass tube expoxied into a 2.5 cm section of hexagonal brass stock that was milled out and tapped for the microphone. Once inserted through the constructed endcap, the maximum length down the resonance tube that could be measured was 28 cm. A second microphone tube was constructed for the series of measurements involving the 2.54 cm stack. This second tube was constructed in the same manner as the first with a length of straight brass tubing of 90.5 cm. The second tube allows measurements down the entire length of the system.

Experimental Setup

In addition to the refrigerator itself, there were several other pieces of equipment used to operate the refrigerator and to take measurements from it. An Agilent Technologies model 33220A waveform generator was used to produce the signal that ran the refrigerator. The stack had an Omega Type K thermocouple attached to each end of it to measure the temperature. These were connected to an Omega HH501DK Type K thermocouple reader. An Endevco model 8510B-1 piezoresistive pressure tranducer, hereafter referred to as the microphone, was used to measure the pressure in the system. The microphone was connected to a "black box" which is on loan from the University of Mississippi. The "black box" conditions and amplifies the signal from the microphone. The conditioned signal is then routed into an Agilent Technologies DSO3062A oscilloscope. It is from the oscilloscope data that the pressure inside the system was calculated.

The first configuration for the system involved connecting the waveform generator to the driver box, without any intervening equipment. The second configuration (see figure D.10) was similar to the first except that the waveform generator signal was routed through an AudioSource Model AMP One/A stereo power amplifier, then through two GoldStar DM-31 multimeters before it reached the driver box. This configuration allow for more power input to the driver and a way to measure that power.

Methodology

The first phase was to find the resonance frequency of the system. For each of the configurations, this involved using the waveform generator to drive the system at different frequencies and recording the resulting voltage outputs from the microphone. This was done without a stack in place.

The program GNUplot was then used to fit this data to equation (B.7) to find the quality factor and resonance frequency (see figure D.16). The second phase involved holding the power input constant, but varying the position of the 5.23 cm stack. The third phase involved placing the 5.23 cm stack in one position in the resonator and varying the power of the signal sent to the driver. The final phase repeated the second phase using the 2.54 cm stack.

Results and Analysis

Using equation (11) and the length of the glass pipes used as a resonator (0.44 m), we calculate the fundamental frequency of the system to be

$$f_0 = \frac{\nu}{4L} = \frac{347.21 \text{m/s}}{4 \times 0.44 \text{m}} = 197.3 \text{Hz}, \tag{13}$$

which differed from the experimentally determined frequency. The experimental frequency of 169.8Hz was found by numerically fitting the data to equation(B.7) (see figure D.16). The reason for the discrepency is the gap that exists between the end of the resonance tube and the surface of the driver. This gap makes the effective length of the resonance tube slightly longer, thus lowering the frequency.

Using the experimentally determined frequency, we can use properties of air at standard temperature and pressure, via equation (12) to calculate the thermal penetration depth.

$$\delta_\kappa = \sqrt{\frac{\kappa}{\pi f \rho c_p}} = \sqrt{\frac{0.02624 \text{ W/(m K)}}{\pi \times (1.173 \text{ kg/m}^3) \times (169.8 \text{ Hz}) \times (1005 \text{ J/(m K)})}} = 0.204 \text{ mm} \tag{14}$$

Which is about fourteen percent (14%) of the radius of a pore.

Initial data runs conducted with a 2.54 cm stack resulted in a temperature gradient which was expected, however heat was building up in the system. Although a constant temperature gradient could be achieved, the temperature of the "cold" side of the stack underwent a continual increase.

A heat exchanger was added to the system and the 5.23 cm stack was utilized. Each data point was taken after 10 minutes of operation, then the system was allowed to cool down before taking the next data point. Inspection of the data (see table C.2 and figure D.11) revealed that heat was building up in the water being recycled in the heat exchanger. Even though there was an overall increase in the temperature of the system, a temperature gradient was maintained from one end of the stack to the other. The maximum gradient of 7.8°C was achieved when the stack was positioned so that its upper end was 7 cm from the closed end of the resonator tube. The calculated coefficient of performance (see equation (9)) at the 7 cm position was 0.0028 and 0.017% of Carnot performance

Carefully controlled introduction of ice into the recycled water was used to maintain a constant temperature on the "hot" end of the stack. This prevented a buildup of heat in the system, allowing it to equilibrate more readily between data points. Again, each data point was taken after 10 minutes of operation. As in the previous trial, the maximum temperature gradient was achieved at the 7 cm mark (see table C.3 and figure D.14), but this time it was 12.6°C. While there was an increase in temperature gradient and a lower T_L, some performance was sacrificed. The calculated coefficient of performance was only 0.00183, and only 0.008% of Carnot.

Placing the stack at the 7 cm mark, a frequency sweep was made from 20Hz on either side of the resonance frequency (see figure D.17). The results show that as the frequency is shifted away

from the resonance frequency, the temperature gradient drops as the pressure of the standing wave drops.

The 5.23 cm stack was replaced with 2.54 cm stack and another set of data points was taken using the same method of run time and cool down. This time a Thermo Scientific NESLAB RTE7 refrigerated bath was used to hold the heat exchanger at a constant temperature. The calculated coefficient of performance for this arrangement was 0.00403 and only 0.017% of Carnot.

Conclusion

Thermoacoustic refrigeration using air as the operating gas performs poorly when compared to Carnot's coefficient of performance. While other researchers have achieved better results using other gasses and different construction materials, their performance also falls well below those of vapor compression systems, which can be more than 50% of Carnot[8]. Despite the lesser performance, further exploration of thermoacoustic systems is warranted by their greater reliability. There are several avenues for future research with this refrigerator, changes in stack length and variations in power settings are merely two possible explorations being presently considered.

The Appendices that follow contain figures and data pertinent to the experiments performed with the demonstration model thermoacoustic refrigerator, as well as some other research work done to establish some fundamental background in the area of thermoacoustics.

APPENDIX

- **A:** Calibration of microphone, power supply and signal conditioner that allowed conversion of electrical power data into pressure values.

- **B:** Quality Factor derivation. While the quality factor was not considered important for this research, the derived equation was fitted to the data to find the resonance frequency of the system.

- **C:** Data tables of data taken for the experiments.

- **D:** Figures of concepts, diagrams and pictures of the the refrigerator and its parts, and graphs of the data from Appendix C.

- **E:** Derivation of equation for stack placement for maximum work output for a prime mover.

- **F:** Derivation of η/η_{max} and comparing it to the results from Swift's paper[6], including plots of the differences with $\dot{W}/\dot{W}_{max}$ with the script files necessary to generate the plots.

- **G:** General background research into thermoacoustic prime mover efficiencies compared to conventional engines.

- **H:** General background research into coefficient of performance for conventional and thermoacoustic refrigerators.

Appendix A

Microphone/Black Box calibration

Calibration of the microphone and the "black box", which amplifies and conditions the signal, was accomplished using a known sound source. In this case, the sound source was a model CA250, Precision Acoustic Calibrator. When activated, the calibrator emits sound 114 dB SPL with a frequency of 250 Hz. Several readings were taken for each plug and each microphone, and the results were averaged and appear in table A.1

| Microphone Serial Number | Black Box Plug (as viewed from back side) | | | | | |
| | A (left) | | B (center) | | C (right) | |
	Reading (mV)	Conversion Factor (Pa/mV)	Reading (mV)	Conversion Factor (Pa/mV)	Reading (mV)	Conversion Factor (Pa/mV)
11579	4.721	3.00269	4.721	3.00269	4.721	3.00269
11331	4.641	3.05445	4.641	3.05445	4.641	3.05445
11314	5.601	2.53093	5.601	2.53093	5.601	2.53093

Table A.1: Microphone Voltage to Pressure via the "Black Box"

Appendix B

Derivation of Quality Factor

For the equation of motion of a damped driven oscillator, $\ddot{x} + 2\beta\dot{x} + \omega_0^2 x = \mathrm{F}e^{i\omega t}$, we get the solution for the amplitude:

$$A = \frac{\mathrm{F}}{\omega_0^2 - \omega^2 + 2i\beta\omega} \tag{B.1}$$

To get the absolute value of A, we take the square root of A^*A

$$\begin{aligned}
|A| &= \sqrt{A^*A} \\
&= \sqrt{\left(\frac{\mathrm{F}}{\omega_0^2 - \omega^2 - 2i\beta\omega}\right)\left(\frac{\mathrm{F}}{\omega_0^2 - \omega^2 + 2i\beta\omega}\right)} \\
&= \sqrt{\frac{\mathrm{F}^2}{\omega_0^4 - 2\omega_0^2\omega^2 + \omega^4 + 4\beta^2\omega^2}} \\
&= \frac{\mathrm{F}}{\sqrt{(\omega_0^2 - \omega^2)^2 + 4\beta^2\omega^2}} \tag{B.2}
\end{aligned}$$

Making the substitution $\beta = b/2m$, we get

$$|A| = \frac{\mathrm{F}}{\sqrt{(\omega_0^2 - \omega^2)^2 + \frac{b^2}{m^2}\omega^2\frac{\omega_0^4}{\omega_0^4}}} \tag{B.3}$$

Then using the substitution $Q = \omega_0 m/b$, where Q is the quality factor, we get:

$$|A| = \frac{\mathrm{F}}{\sqrt{\left[\omega_0^2\left(1 - \frac{\omega^2}{\omega_0^2}\right)\right]^2 + \frac{\omega_0^4\omega^2}{Q^2\omega_0^2}}}$$

Factoring out an ω_0^4/Q^2 out of both terms in the radical, we get:

$$|A| = \frac{\mathrm{F}}{\sqrt{\frac{\omega_0^4}{Q^2}\left[Q^2\left(1 - \frac{\omega^2}{\omega_0^2}\right)^2 + \frac{\omega^2}{\omega_0^2}\right]}} \tag{B.4}$$

Further factoring out an ω^2/ω_0^2 out of the terms under the radical and then reducing and reordering them, we get:

$$|A| = \frac{FQ}{\omega_0\omega\sqrt{1 + Q^2\frac{\omega^2}{\omega_0^2}\left(1 - \frac{\omega_0^2}{\omega^2}\right)^2}} \tag{B.5}$$

This equation has it's maximum when $\omega = \omega_0$. This gives us an $A_{\max}$ of

$$A_{\max} = \frac{FQ}{\omega_0\omega} = \frac{FQ}{\omega_0^2} = \frac{F\omega_0 m}{b\omega_0^2} = \frac{F}{2\beta\omega_0} \tag{B.6}$$

Dividing equation (B.5) by equation (B.6), we get the relationship of amplitude to the maximum amplitude. The frequency (f) can be substituted for the angular frequency (ω) as all of the 2π's cancel out, leaving us with

$$\frac{|A|}{A_{\max}} = 1/\sqrt{1 + Q^2\frac{f^2}{f_0^2}\left(1 - \frac{f_0^2}{f^2}\right)^2} \tag{B.7}$$

Appendix C

Tables

In the following tables the values of position (x), temperatures, microphone signal strength (V_{pp}), and the rms voltage and current sent to the driver (V_{RMS} and I_{RMS}) were measured quantities. P_{AC} was calculated based on the V_{pp} and the calibration in Table A.1. The acoustic power sent to the driver (P) was calculated by converting V_{RMS} and I_{RMS} into V and I, and using the equation $P = I \, V$. Q_I is calculated using equation 7. COP is calculated using the basic benefit/cost using Q_I as the benefit and P as the cost. COP_C is calculated using the final temperatures in equation 6. COPR is calculated by dividing COP by COP_C.

	Initial		Final										
x	T_L	T_0	T_L	T_0	V_{pp}	V_{RMS}	I_{RMS}	P_{AC}	P	Q_I	COP	COP_C	COPR
(cm)	(°C)	(°C)	(°C)	(°C)	(V)	(V)	(A)	(kPa)	(W)	(mW)			
3	22	23.2	15.8	20.7	2.901	8.84	0.63	4.355	11.14	9.	8.0E-4	58.97	1.0E-5
4	22.4	25	14.3	28.3	2.901	8.84	0.64	4.355	11.32	26.	2.3E-3	20.53	1.1E-4
5	22	26	12.5	29.1	2.881	8.85	0.65	4.325	11.51	30.	2.6E-3	17.21	1.5E-4
6	22	26.5	12.2	29.7	2.881	8.85	0.66	4.325	11.68	32.	2.7E-3	16.31	1.7E-4
7	22.1	27	12.3	30.1	2.861	8.85	0.67	4.295	11.86	33.	2.8E-3	16.04	1.7E-4
8	22	27.2	12.4	30.1	2.841	8.85	0.69	4.265	12.21	32.	2.6E-3	16.13	1.6E-4
9	21.9	27.3	13.5	30.1	2.781	8.83	0.70	4.175	12.36	30.	2.4E-3	17.27	1.4E-4

Table C.1: Each data point taken 10 minutes after starting refrigerator. The 5.23 cm stack in use. Water recirculation pump was used, without controlling the water temperature.

| | Initial | Final | | | | | | | | | | |
x (cm)	T_L (°C)	T_L (°C)	T_0 (°C)	V_{pp} (V)	V_{RMS} (V)	I_{RMS} (A)	P_{AC} (kPa)	P (W)	Q_I (mW)	COP	COP_C	COPR
3	19.7	12.1	19.9	2.961	8.87	0.67	4.445	11.89	14	1.18E-3	36.57051	3.0E-5
4	19.4	9.6	19.8	2.921	8.87	0.67	4.385	11.89	19	1.6E-3	27.72059	6.0E-5
5	18.7	7.9	20	2.901	8.87	0.68	4.355	12.06	22	1.82E-3	23.22727	8.0E-5
6	16.4	7.5	19.9	2.901	8.87	0.7	4.355	12.42	23	1.85E-3	22.63306	8.0E-5
7	16.6	7.4	20	2.861	8.87	0.71	4.295	12.6	23	1.83E-3	22.26587	8.0E-5
8	16.5	7.8	20	2.861	8.87	0.72	4.295	12.77	22	1.72E-3	23.02869	7.0E-5
9	16.9	8.4	19.9	2.861	8.87	0.72	4.295	12.77	21	1.64E-3	24.48261	7.0E-5
10	17	8.9	19.9	2.781	8.86	0.74	4.175	13.11	20	1.53E-3	25.64091	6.0E-5
11	17.1	9.2	19.9	2.701	8.85	0.75	4.055	13.28	20	1.51E-3	26.38785	6.0E-5
12	17.2	9.9	20	2.661	8.85	0.77	3.995	13.63	19	1.39E-3	28.02475	5.0E-5
13	17	10.7	20	2.581	8.85	0.78	3.875	13.81	17	1.23E-3	30.52151	4.0E-5
14	17.2	11.4	20	2.501	8.84	0.79	3.755	13.97	16	1.15E-3	33.08721	3.0E-5
15	17.3	11.9	20	2.481	8.83	0.8	3.725	14.13	15	1.06E-3	35.19136	3.0E-5
16	17.2	12.2	20	2.421	8.84	0.82	3.635	14.5	14	9.7E-4	36.58333	3.0E-5
17	18.3	13.2	20	2.301	8.83	0.82	3.455	14.48	12	8.3E-4	42.11029	2.0E-5

Table C.2: Each data point taken 10 minutes after starting refrigerator. The 5.23 cm stack in use. Water recirculation pump was used, periodic introduction of ice into the water reservoir to maintain constant T_0.

x (cm)	Final T_L (°C)	Final T_0 (°C)	V_pp	V_RMS	I_RMS (A)	P_AC (kPa)	P (W)	Q_I (mW)	COP	COP_C	COPR
5	8	20	2.921	8.63	0.632	4.385	10.91	44	4.03E-3	23.42917	1.72E-4
6	9	20	2.921	8.62	0.634	4.385	10.93	4	3.66E-3	25.65	1.427E-4
7	10	20	2.921	8.63	0.635	4.385	10.96	37	3.38E-3	28.315	1.194E-4
8	10	20	2.901	8.58	0.641	4.355	11	37	3.36E-3	28.315	1.187E-4
9	10	20	2.901	8.55	0.645	4.355	11.03	37	3.35E-3	28.315	1.183E-4
10	10	20	2.881	8.54	0.65	4.325	11.1	37	3.33E-3	28.315	1.176E-4
11	10	20	2.861	8.53	0.655	4.295	11.17	37	3.31E-3	28.315	1.169E-4
12	11	20	2.841	8.54	0.66	4.265	11.27	33	2.93E-3	31.57222	9.28E-5
13	12	19	2.821	8.5	0.75	4.235	12.75	26	2.04E-3	40.73571	5.01E-5
14	12	20	3.041	9.62	0.75	4.566	14.43	29	2.01E-3	35.64375	5.64E-5
15	13	20	2.941	9.08	0.71	4.415	12.89	26	2.02E-3	40.87857	4.94E-5
16	13	20	2.881	9.12	0.73	4.325	13.32	26	1.95E-3	40.87857	4.77E-5
17	14	20	2.861	9.2	0.75	4.295	13.8	22	1.59E-3	47.85833	3.32E-5
18	15	20	2.821	9.16	0.76	4.235	13.92	18	1.29E-3	57.63	2.24E-5
19	15	20	2.781	9.2	0.76	4.175	13.98	18	1.29E-3	57.63	2.24E-5
20	16	20	2.741	9.22	0.77	4.115	14.2	15	1.06E-3	72.2875	1.47E-5
21	16	20	2.721	9.18	0.78	4.085	14.32	15	1.05E-3	72.2875	1.45E-5
22	16	20	2.681	9.25	0.79	4.025	14.62	15	1.03E-3	72.2875	1.42E-5
23	17	20	2.641	9.25	0.8	3.965	14.8	11	7.4E-4	96.71667	7.7E-6
24	17	20	2.601	9.23	0.8	3.905	14.77	11	7.4E-4	96.71667	7.7E-6
25	17	20	2.521	9.23	0.81	3.785	14.95	11	7.4E-4	96.71667	7.7E-6
26	17	20	2.461	9.1	0.8	3.695	14.56	11	7.6E-4	96.71667	7.9E-6
27	18	20	2.421	9.11	0.81	3.635	14.76	7	4.7E-4	145.575	3.2E-6
28	18	20	2.381	9.13	0.81	3.575	14.79	7	4.7E-4	145.575	3.2E-6
29	18	20	2.341	9.15	0.82	3.515	15.01	7	4.7E-4	145.575	3.2E-6
30	18	20	2.141	8.91	0.83	3.214	14.79	7	4.7E-4	145.575	3.2E-6
31	18	20	2.081	8.83	0.83	3.124	14.66	7	4.8E-4	145.575	3.3E-6

Table C.3: Each data point taken 10 minutes after starting refrigerator. The 2.54 cm stack in use. Temperature regulated recirculation pump was used to maintain constant T_0.

Position (cm)	Final		V_{pp}	V_{RMS}	I_{RMS} (A)	P_{AC} (kPa)	P (W)	Q_I (mW)	COP	COP_C	COPR
	T_L (°C)	T_0 (°C)									
32	18	20	2.061	8.97	0.83	3.094	14.89	7	4.7E-4	145.575	3.2E-6
33	18	20	2.101	9	0.81	3.154	14.58	7	4.8E-4	145.575	3.3E-6
34	18	20	1.981	8.97	0.84	2.974	15.07	7	4.6E-4	145.575	3.2E-6
35	18	20	1.961	9	0.85	2.944	15.3	7	4.6E-4	145.575	3.2E-6
36	19	20	1.921	8.95	0.85	2.884	15.22	4	2.6E-4	292.15	9.0E-7
37	19	20	1.881	8.9	0.84	2.824	14.95	4	2.7E-4	292.15	9.0E-7
38	19	20	1.861	8.95	0.85	2.794	15.22	4	2.6E-4	292.15	9.0E-7
39	19	20	1.821	8.87	0.85	2.734	15.08	4	2.7E-4	292.15	9.0E-7
40	20	20	1.801	8.97	0.86	2.704	15.43	0	0	——	——
41	20	20	1.801	9.09	0.87	2.704	15.82	0	0	——	——
42	20	20	1.781	9.06	0.87	2.674	15.76	0	0	——	——
43	20	20	1.761	9.06	0.87	2.644	15.76	0	0	——	——
44	20	20	1.741	9.01	0.87	2.614	15.68	0	0	——	——

Table C.4: Continuation of data in Table C.3

Appendix D

Figures
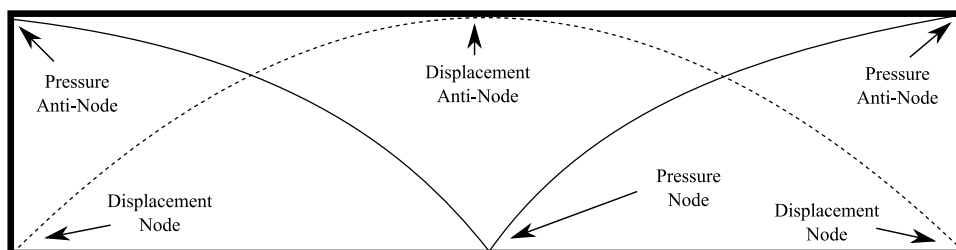
Figure D.1: **Pressure and Displacement Amplitudes in a Straight Pipe Resonator**
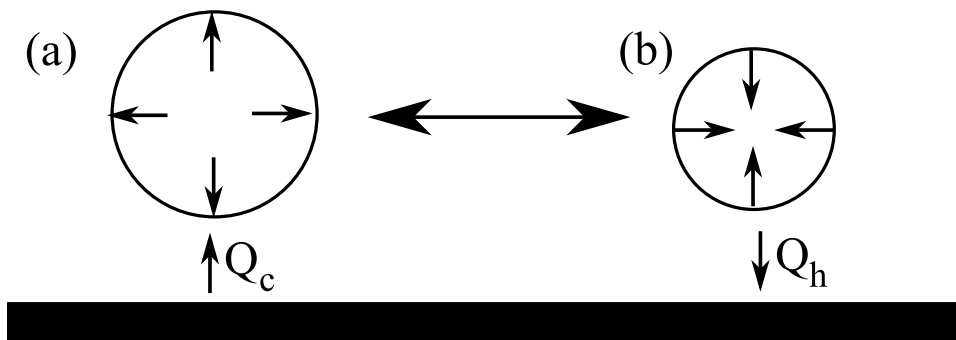
Figure D.2: **Gas Parcel moving Heat**
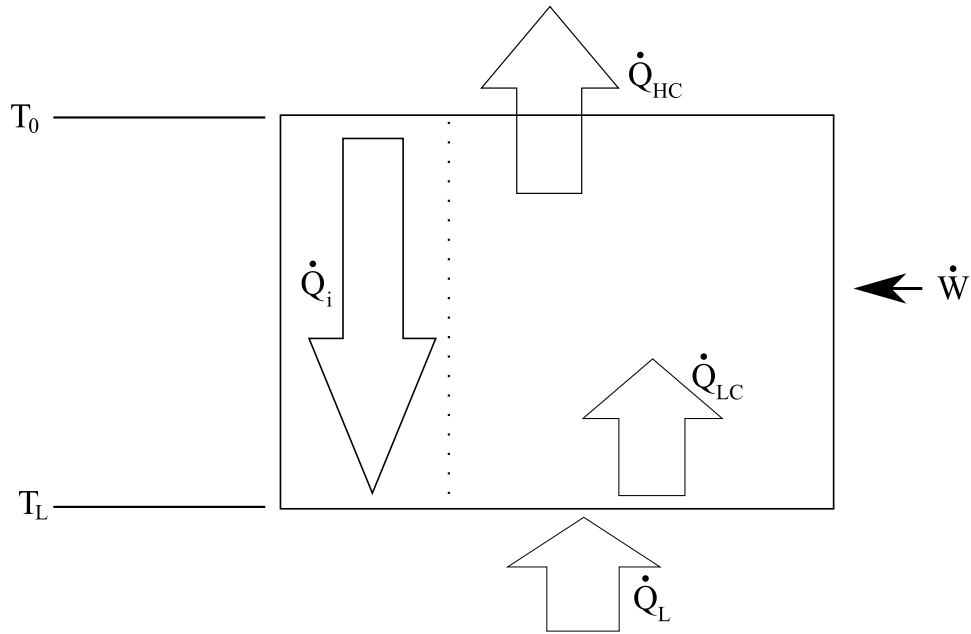
Figure D.3: **Heat Flow in a Refrigerator**. $\dot{Q}_{HC}$ is the rate of heat flowing out of the refrigerator into the hot reservoir. $\dot{Q}_L$ is the rate of heat flowing into the system from the cold reservoir. $\dot{Q}_i$ is the rate of heat leaking into the refrigerator. $\dot{Q}_{LC}$ it the rate of heat being moved at the rate of work ($\dot{W}$).
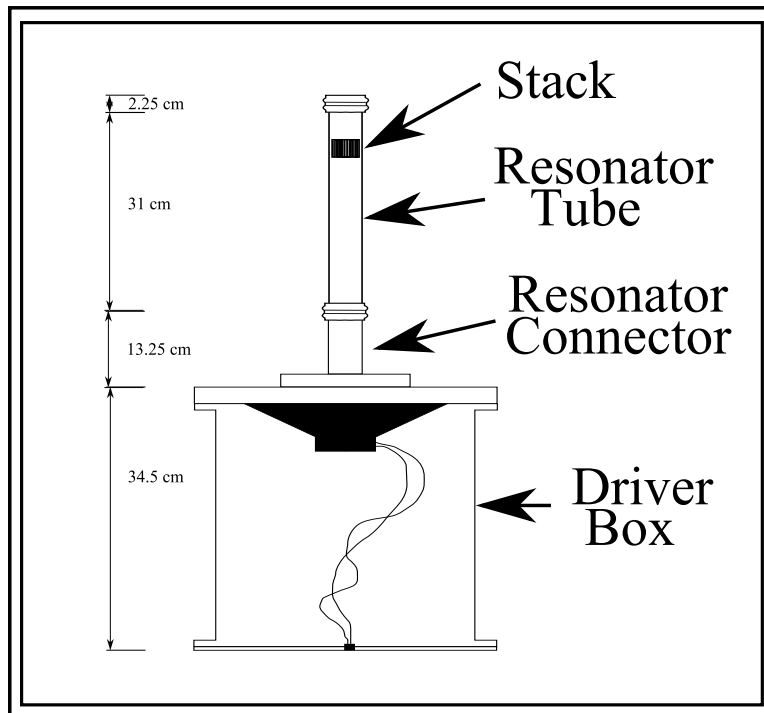
Figure D.4: **Straight Pipe Configuration**

(a)   (b)
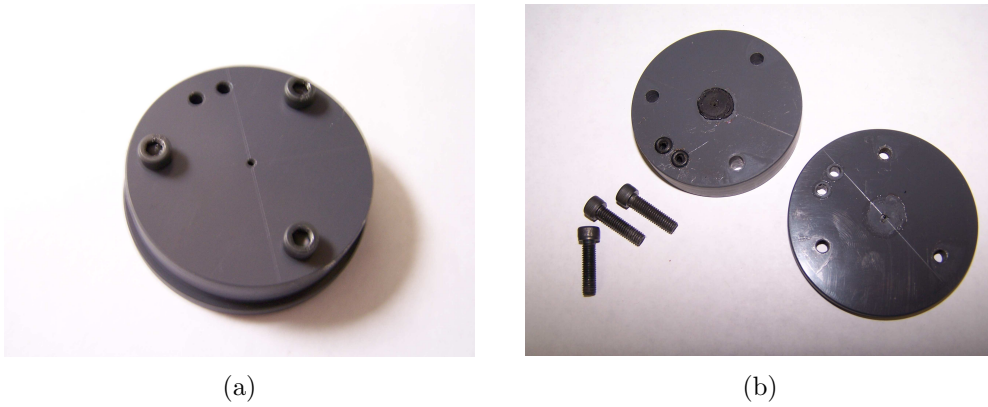
Figure D.5: **Endcap**
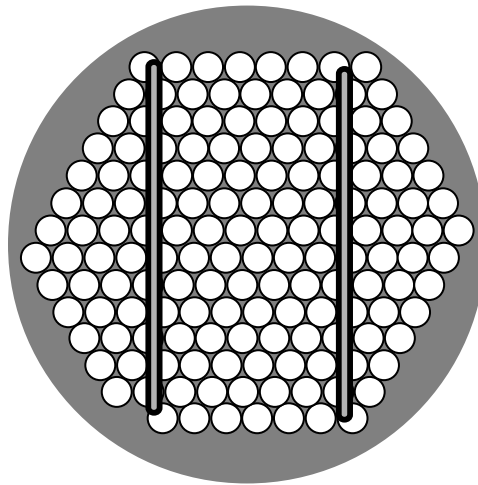
Figure D.6: **Porosity**: Total porosity is represented by everything inside the large gray circle. The toothpicks are represented by the two outlined rectangles cutting across the small circles. Open area is represented by the small white circles.
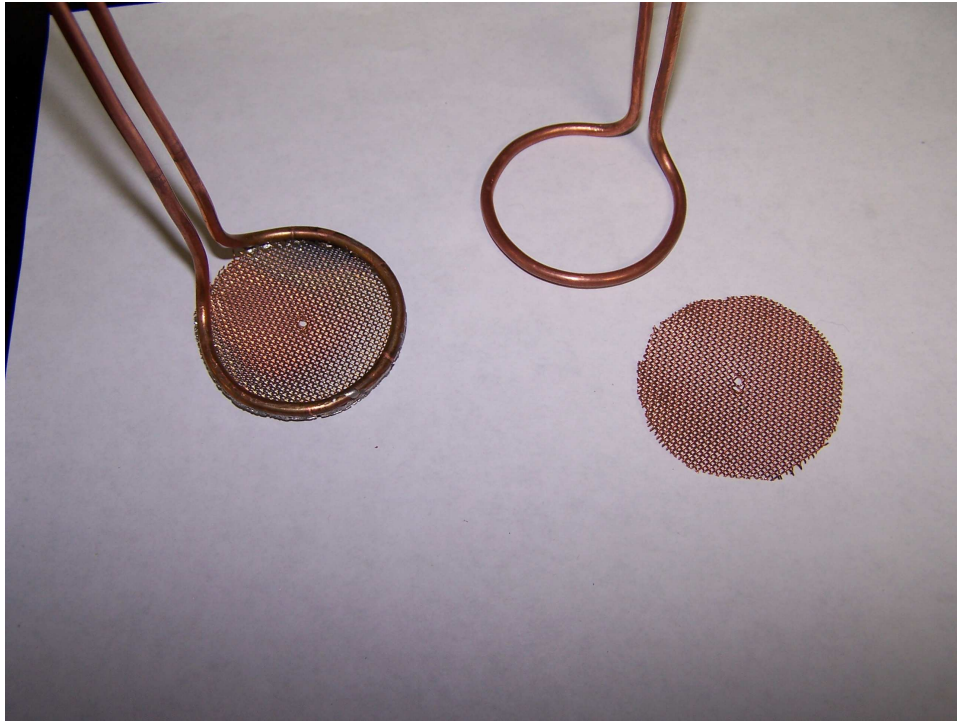
Figure D.7: **Heat Exchanger**: On the left is the completed heat exchanger. On the right are the copper tubing and copper screen mesh components that make up the completed heat exchanger.

(a) 2.54 cm long Cocktail Straw Stack (b) 5.23 cm long Cocktail Straw Stack

Figure D.8: Cocktail Straw Stacks. Each stack is composed of same number of pores each consisting of a plastic cocktail straw with an inner diameter of 2.85 mm, resulting in a diameter of 4.74 cm and a porosity (Ω) of 0.619
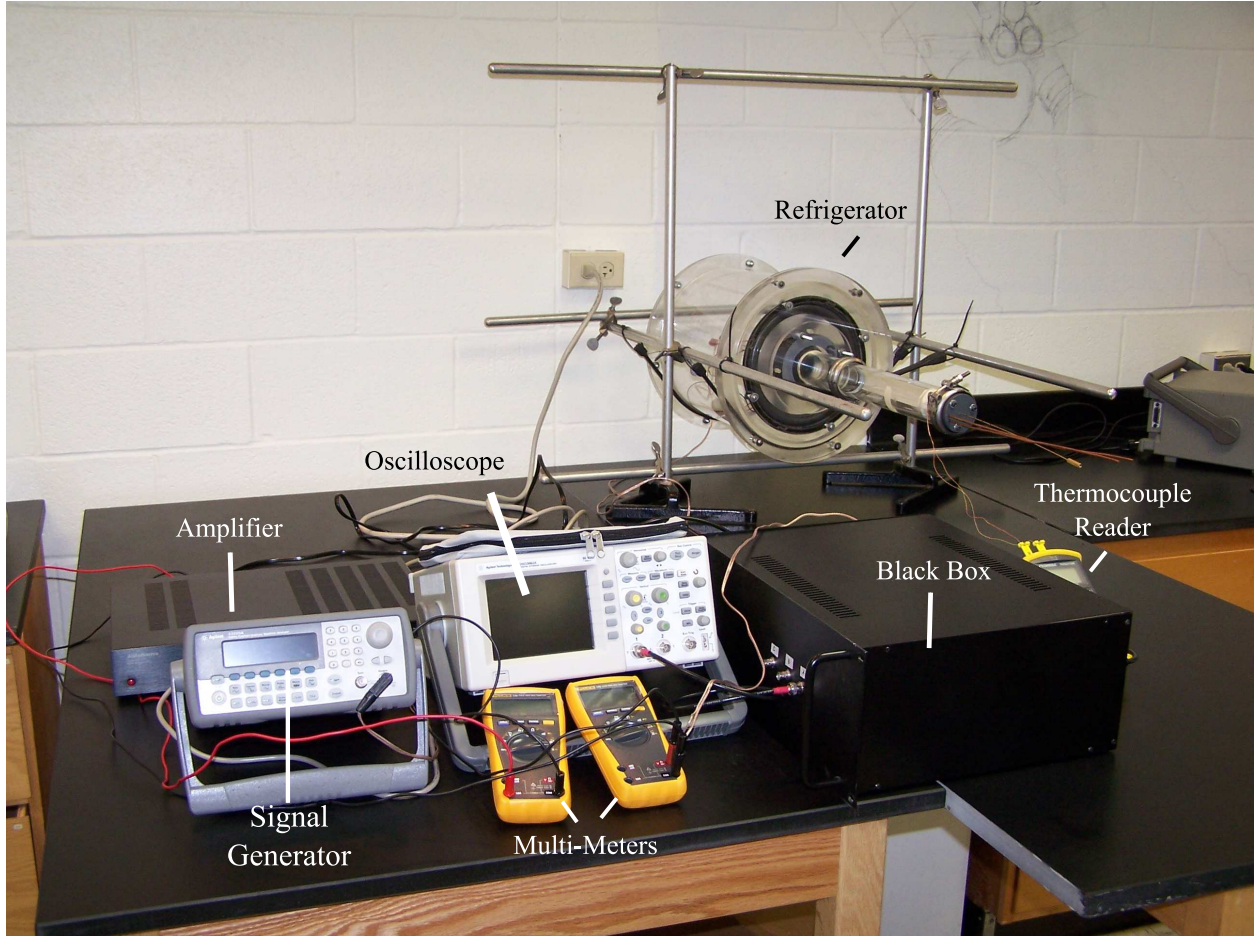
Figure D.9: Photograph of the refrigerator with its auxillary equipment.
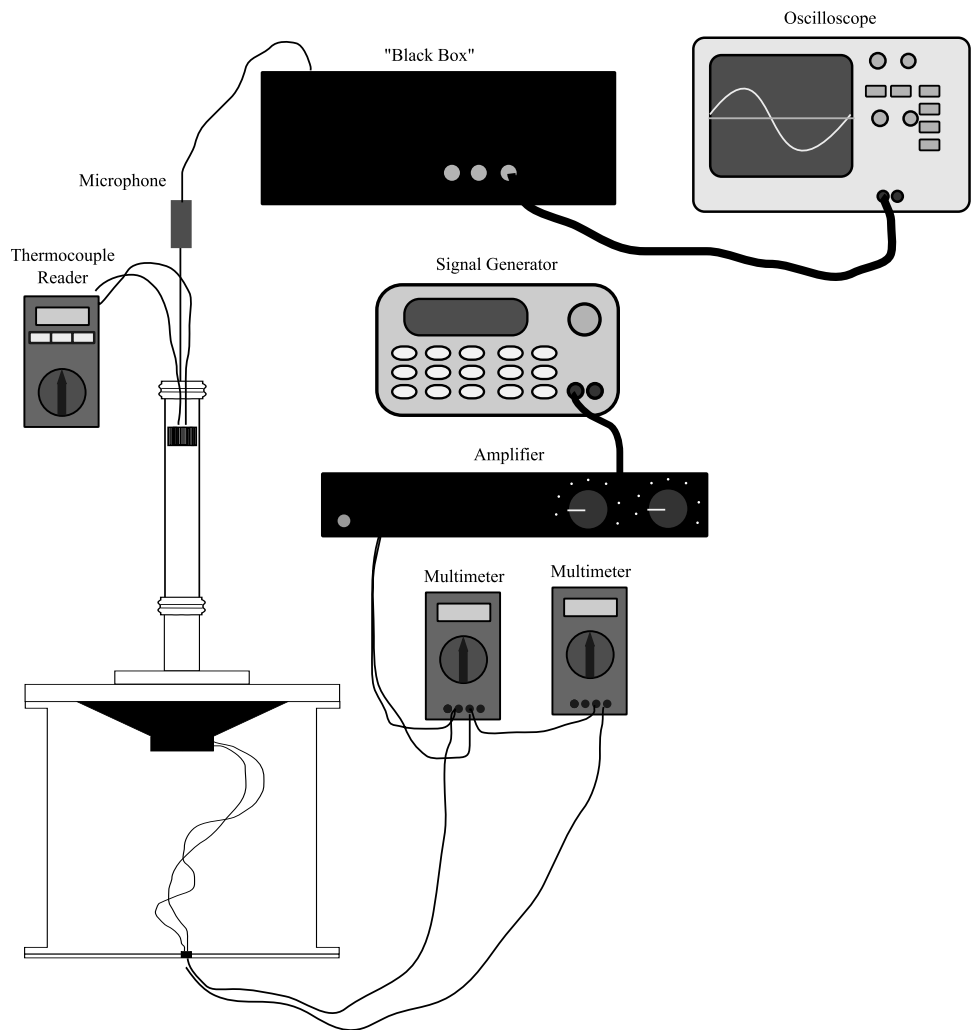
Figure D.10: **System Configuration**
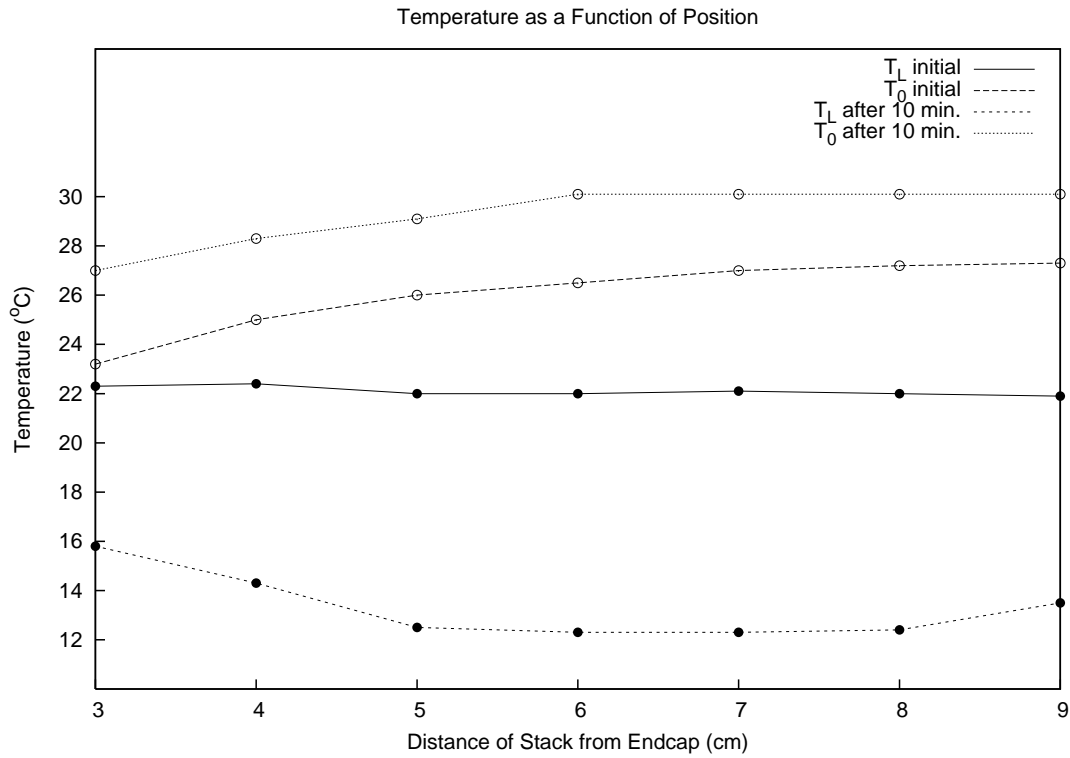
Figure D.11: **ΔT as a function of position without temperature controlling recirculating water.** 5.23cm Stack in use.
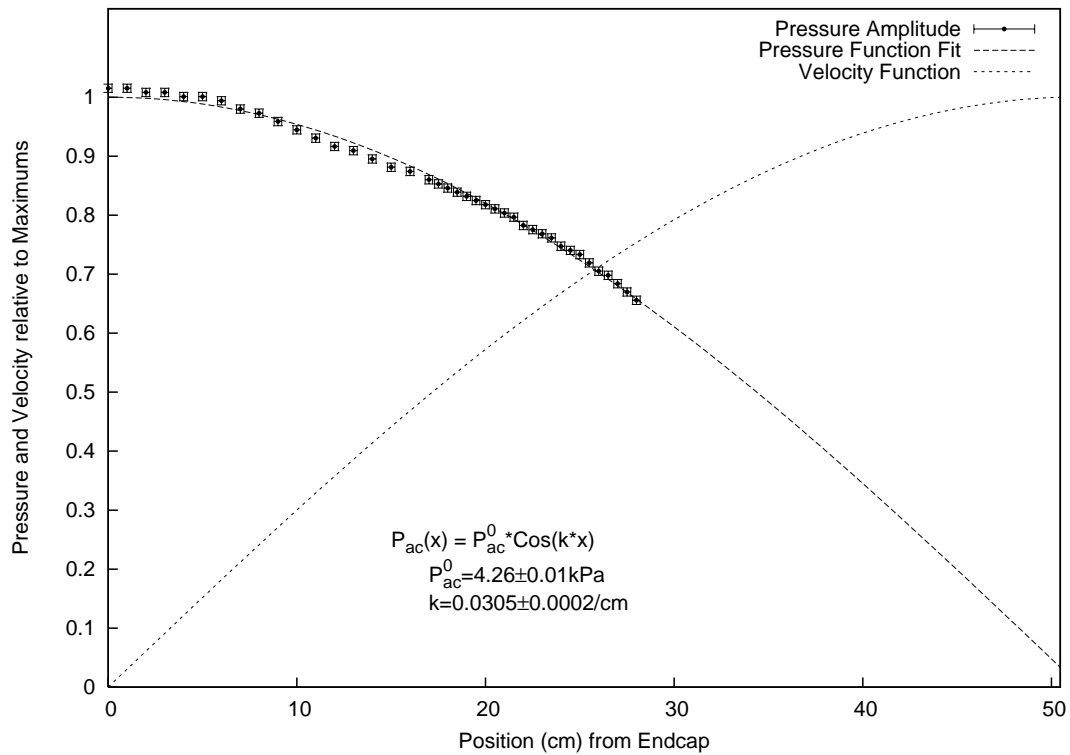
Figure D.12: **Pressure and Velocity as a function of Position.** 5.23cm Stack in use with short microphone tube.
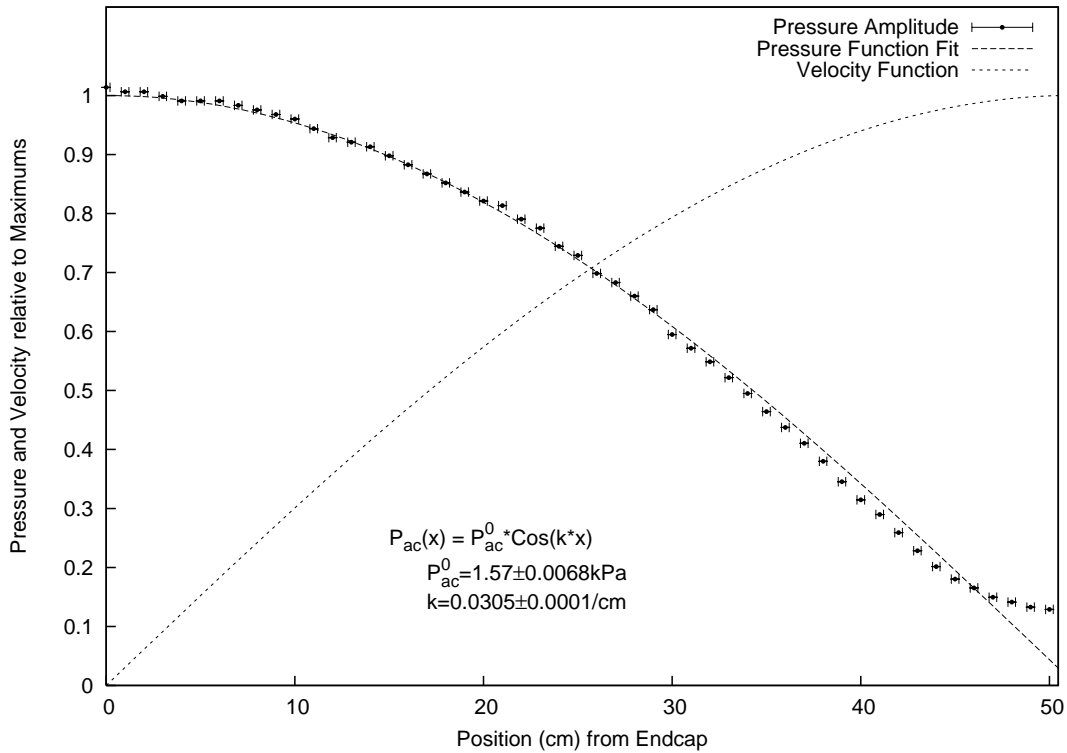
Figure D.13: **Pressure and Velocity as a function of Position.** 2.54cm Stack in use with long microphone tube. The data for this graph was taken at a lower power setting and does not appear in the appendices.
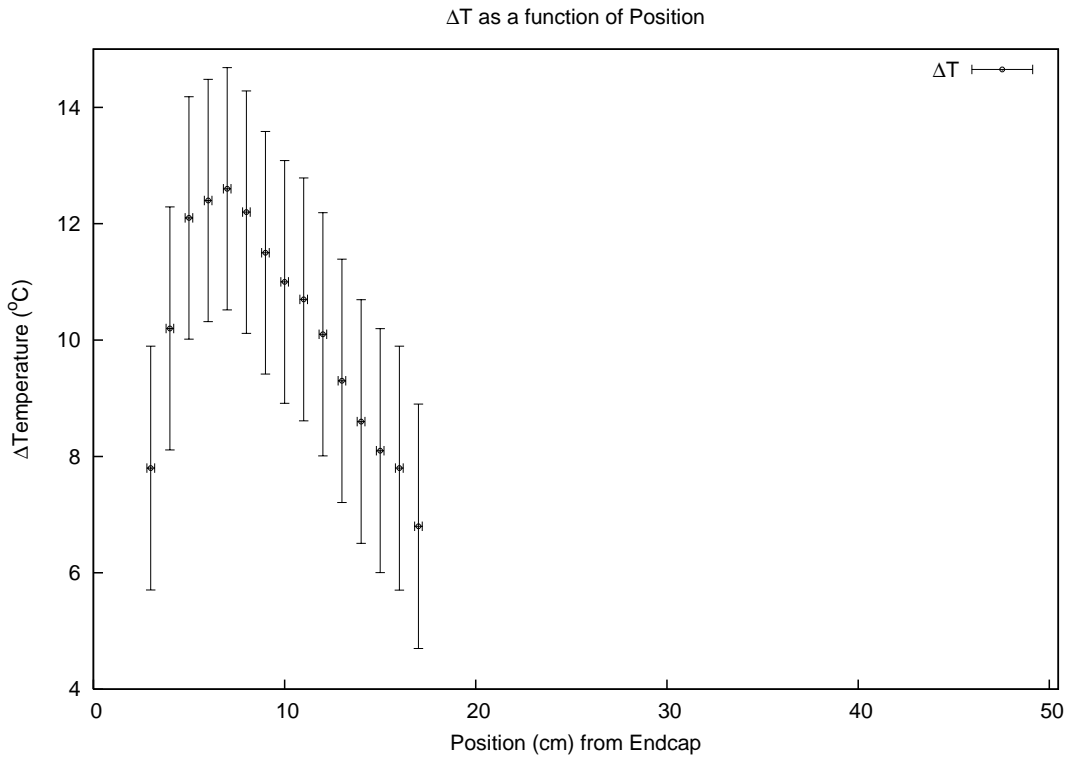
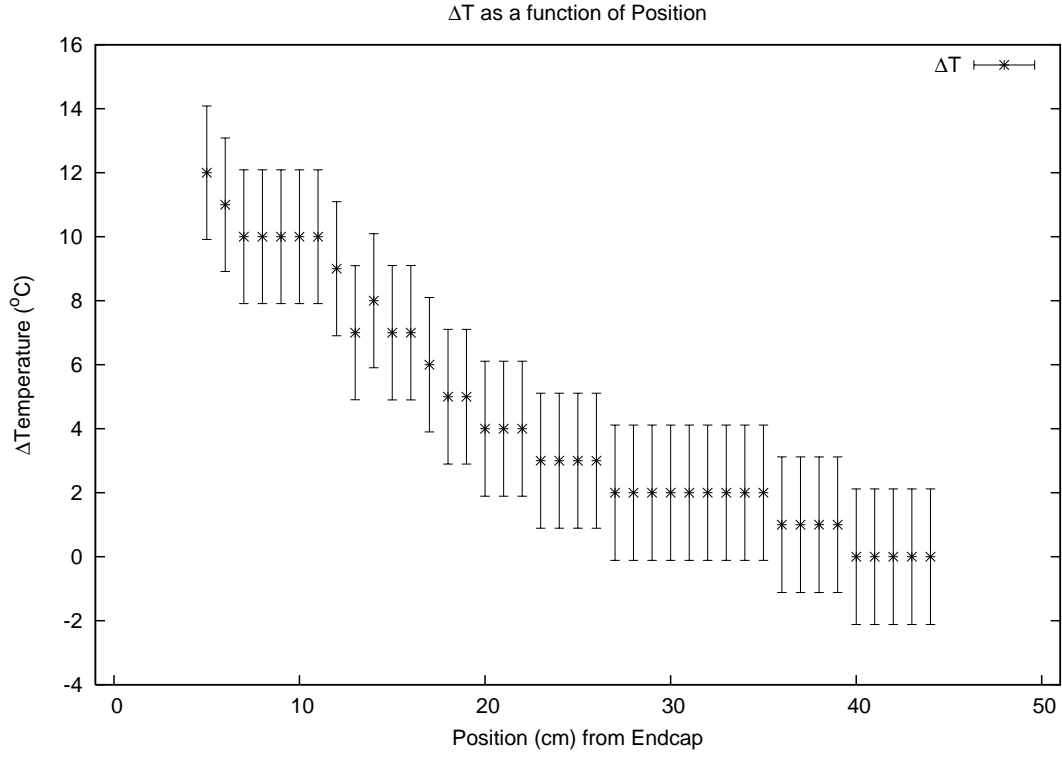Figure D.14: **ΔT as a function of Position.** 5.23cm Stack in use.

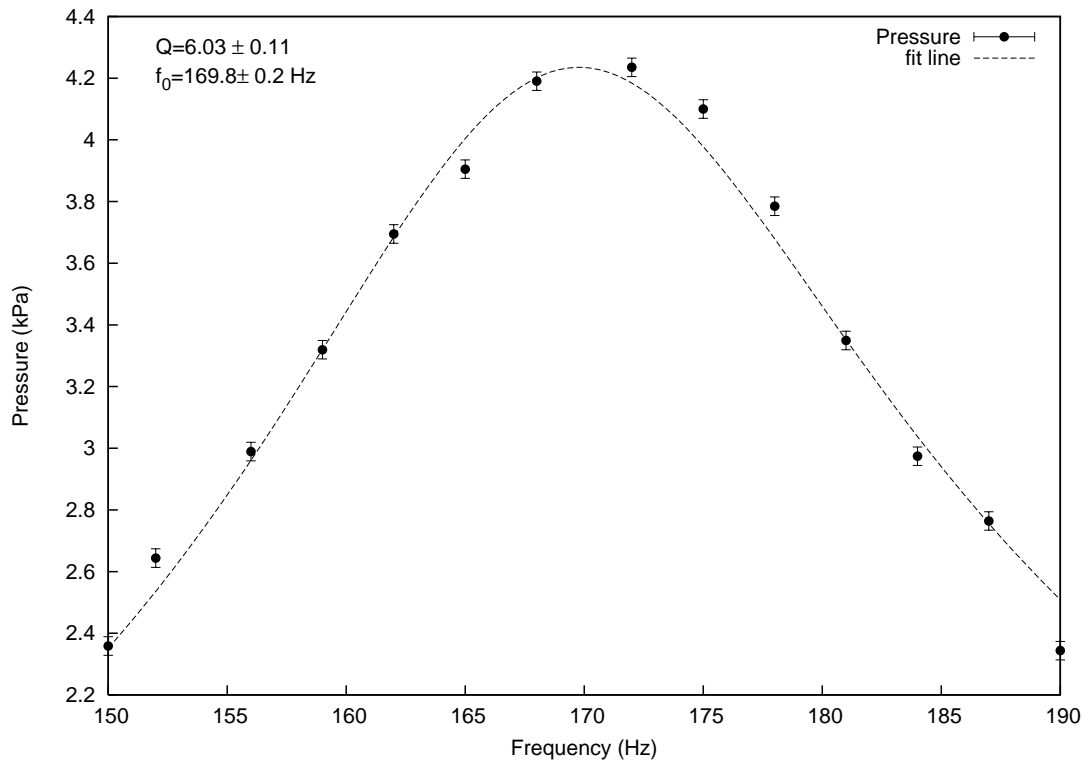Figure D.15: **ΔT as a function of Position.** 2.54cm Stack in use.

Figure D.16: **Pressure as a function of Frequency.** 5.23cm Stack in use.
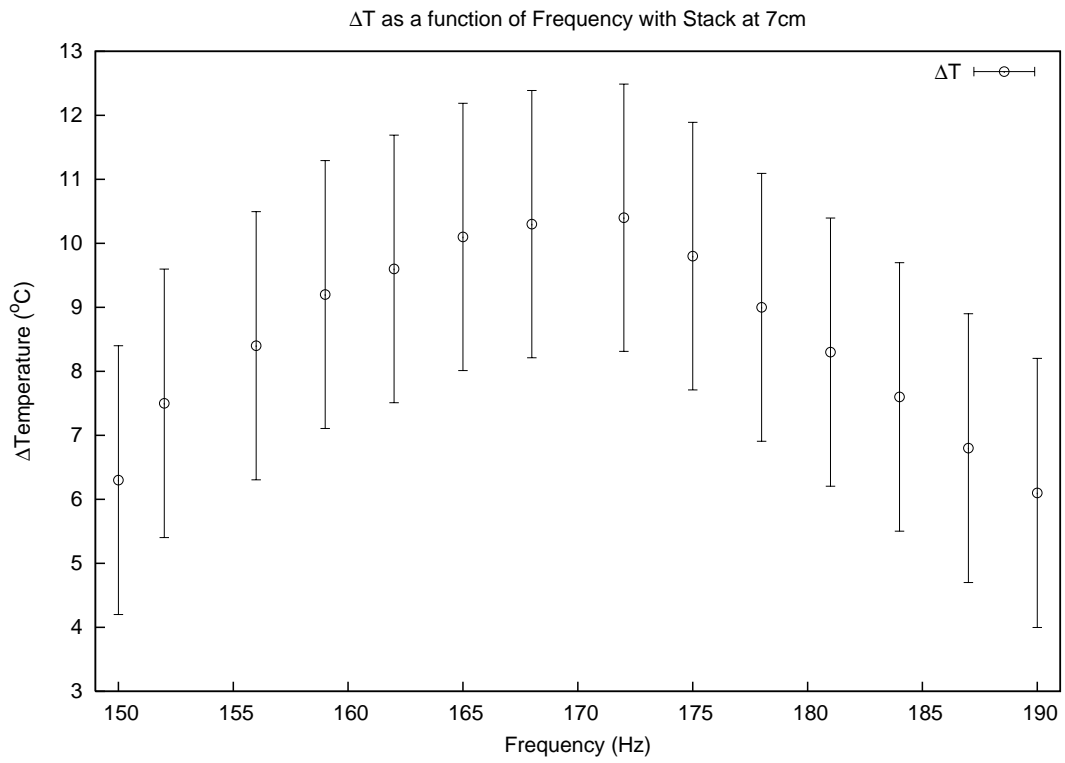
Figure D.17: **ΔT as a function of Frequency.** 5.23cm Stack in use.

Appendix E

Derivation of $x_{max}\left[T_{0_z}\right]$

Starting with Arnott's[12] Equation (65) for work.

$$\overline{\dot{W}}_2[z] = \frac{A_{res}\Omega}{2}P_1[L]^2\frac{T_0\beta^2\omega d}{\rho_0 c_p}\mathrm{Im}\left[F^*\left(\lambda_T\right)\right]\cos^2\left[k_0(L-z)\right](1-\Gamma)$$

where Γ is defined as

$$\Gamma = T_{0_z}\frac{c_p}{\omega\Omega\beta T_0 c}tan\left[k_0(L-z)\right]$$

The term $k_0(L-z)$ can be rewritten as $\frac{\pi}{2}(1-x)$, where x represents the non-dimensional quantity z/L. Using this substitution into Arnott's equations, then taking the derivative of the work flow equation in terms of x set equal to zero, yields

$$x_{max}\left[\frac{\mathrm{d}T_0}{\mathrm{d}z}\right] = \frac{1}{\pi}tan^{-1}\left[\frac{c_p}{\omega\Omega\beta T_0 c}\frac{\mathrm{d}T_0}{\mathrm{d}z}\right] \tag{E.1}$$

This equation gives the postion for the stack to yeild the maximum work out for a given temperature gradient.
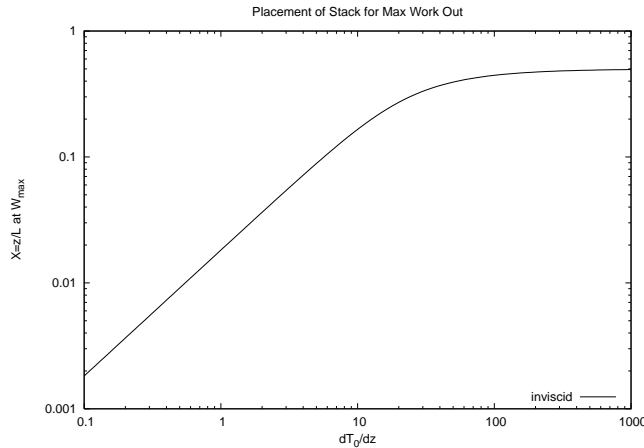

Figure E.1:

Appendix F

Swift's η/η_C and $\dot{W}/\dot{W}_{max}$

Starting with Swift's[6] equation 82 for work:

$$\dot{W}_2 = \frac{1}{4}\Pi\delta_\kappa\Delta x \, \frac{(\gamma-1)\,\omega\,(p_1^s)^2}{(1+\epsilon_s)}\,(\Gamma-1) - \, \Pi\delta_\nu\Delta x \, \omega\rho_m\,\langle u_1^s\rangle^2$$

which by use of $\delta_\nu = \sqrt{\sigma}\delta_\kappa$ will factor to

$$\dot{W}_2 = \frac{1}{4}\Pi\delta_\kappa\Delta x \, \omega\frac{(\gamma-1)\,(p_1^s)^2\,(\Gamma-1)}{\rho_m\,a^2\,(1+\epsilon_s)}\left[1 - \sqrt{\sigma}\frac{(1+\epsilon_s)\,(\rho_m\,a\,\langle u_1^s\rangle\,/p_1^s)^2}{(\gamma-1)\,(\Gamma-1)}\right] \tag{F.1}$$

Moving on to heat, we start with Swift's [6] equation 81:

$$\dot{H}_2 = -\frac{1}{4}\Pi\delta_\kappa\frac{T_m\beta p_1^s\,\langle u_1^s\rangle}{(1+\epsilon_s)\,(1-\sqrt{\sigma})}\,(1-\Gamma) - \Pi\,(y_0 K - lK_s)\frac{\mathrm{d}T_m}{\mathrm{d}x}$$

by use of the substitutions $\mathrm{d}T_m/\mathrm{d}x = \Gamma\nabla T_{crit}$ and $\nabla T_{crit} = T_m\beta p_1^s\omega/\rho_m c_p u_1^s$ this equation will factor to

$$\dot{H}_2 = -\frac{1}{4}\Pi\frac{(\Gamma-1)}{(1+\epsilon_s)\,(1-\sqrt{\sigma})}\delta_\kappa T_m\beta p_1^s\,\langle u_1^s\rangle\left[1 + \frac{4y_0 K\omega}{\delta_\kappa\rho_m c_p\,\langle u_1^s\rangle^2}\frac{(1+lK_s/y_0 K)\,(1+\epsilon_s)\,(1-\sqrt{\sigma})}{(1-1/\Gamma)}\right]$$

looking at the $4y_0 K\omega/\delta_\kappa\rho_m c_p\,\langle u_1^s\rangle^2$, multiplying by 1 in the form of $\delta_\kappa/\delta_\kappa$ and noting that $\delta_\kappa^2 = 2K/\omega\rho_m c_p$ yields $2y_0\delta_\kappa/\left(u_1^s/\omega\right)^2$ which we substitute back into the heat equation resulting in

$$\dot{H}_2 = -\frac{1}{4}\Pi\frac{(\Gamma-1)}{(1+\epsilon_s)\,(1-\sqrt{\sigma})}\delta_\kappa T_m\beta p_1^s\,\langle u_1^s\rangle\left[1 + \frac{2y_0\delta_\kappa}{\left(u_1^s/\omega\right)^2}\frac{(1+lK_s/y_0 K)\,(1+\epsilon_s)\,(1-\sqrt{\sigma})}{(1-1/\Gamma)}\right] \tag{F.2}$$

Combining equations F.1 and F.2 to get efficiency, we get

$$
\begin{aligned}
\eta &= \frac{\dot{W}_2}{\dot{H}_2} \\[2mm]
&= \frac{\frac{1}{4}\Pi\delta_\kappa\Delta x\,\omega\frac{(\gamma-1)\left(p_1^s\right)^2(\Gamma-1)}{\rho_m\,a^2(1+\epsilon_s)}\left[1-\sqrt{\sigma}\frac{(1+\epsilon_s)\left(\rho_m\,a\langle u_1^s\rangle/p_1^s\right)^2}{(\gamma-1)(\Gamma-1)}\right]}{-\frac{1}{4}\Pi\frac{(\Gamma-1)}{(1+\epsilon_s)\left(1-\sqrt{\sigma}\right)}\delta_\kappa T_m\beta p_1^s\langle u_1^s\rangle\left[1+\frac{2y_0\delta_\kappa}{\left(u_1^s/\omega\right)^2}\frac{(1+lK_s/y_0K)(1+\epsilon_s)\left(1-\sqrt{\sigma}\right)}{(1-1/\Gamma)}\right]} \\[2mm]
&= -\frac{\Delta x\,\omega\,p_1^s\,(\gamma-1)\left(1-\sqrt{\sigma}\right)}{\rho_m\,a^2 T_m\beta\langle u_1^s\rangle}\left[\frac{1-\sqrt{\sigma}\frac{(1+\epsilon_s)\left(\rho_m a\langle u_1^s\rangle/p_1^s\right)^2}{(\gamma-1)(\Gamma-1)}}{1+\frac{2y_0\delta_\kappa}{\left(u_1^s/\omega\right)^2}\frac{(1+lK_s/y_0K)(1+\epsilon_s)\left(1-\sqrt{\sigma}\right)}{(1-1/\Gamma)}}\right]
\end{aligned}
$$

substituting in $(\gamma-1)=T_m\beta^2 a^2/c_p$ we get

$$
\eta = -\frac{\Delta x\beta\omega p_1^s}{\rho_m c_p u_1^s}\left(1-\sqrt{\sigma}\right)\left[\frac{1-\sqrt{\sigma}\frac{(1+\epsilon_s)\left(\rho_m a\langle u_1^s\rangle/p_1^s\right)^2}{(\gamma-1)(\Gamma-1)}}{1+\frac{2y_0\delta_\kappa}{\left(u_1^s/\omega\right)^2}\frac{(1+lK_s/y_0K)(1+\epsilon_s)\left(1-\sqrt{\sigma}\right)}{(1-1/\Gamma)}}\right]
$$

Rearranging the equation for ∇T_{crit} we find the relationship $\beta\omega p_1^s/\rho_m c_p u_1^s = \nabla T_{crit}/T_m$ which we substitute in finding the final form for efficiency to be

$$
\eta = -\frac{\Delta x\nabla T_{crit}}{T_m}\left(1-\sqrt{\sigma}\right)\left[\frac{1-\sqrt{\sigma}\frac{(1+\epsilon_s)\left(\rho_m a\langle u_1^s\rangle/p_1^s\right)^2}{(\gamma-1)(\Gamma-1)}}{1+\frac{2y_0\delta_\kappa}{\left(u_1^s/\omega\right)^2}\frac{(1+lK_s/y_0K)(1+\epsilon_s)\left(1-\sqrt{\sigma}\right)}{(1-1/\Gamma)}}\right]
$$

Normalizing the efficiency by dividing it by Carnot's efficiency, where $\eta_C = \Delta T/T_m$ and noting the $1/\Gamma = \Delta x\nabla T_m/\Delta T$ we get the ratio

$$
\frac{\eta}{\eta_C} = -\frac{1}{\Gamma}\left(1-\sqrt{\sigma}\right)\left[\frac{1-\sqrt{\sigma}\frac{(1+\epsilon_s)\left(\rho_m a\langle u_1^s\rangle/p_1^s\right)^2}{(\gamma-1)(\Gamma-1)}}{1+\frac{2y_0\delta_\kappa}{\left(u_1^s/\omega\right)^2}\frac{(1+lK_s/y_0K)(1+\epsilon_s)\left(1-\sqrt{\sigma}\right)}{(1-1/\Gamma)}}\right] \tag{F.3}
$$

This differs from Swift's equation 107 by the leading negative sign and an additional component of:

$$
\sigma\left[\frac{\frac{(1+\epsilon_s)\left(\rho_m a\langle u_1^s\rangle/p_1^s\right)^2}{(\gamma-1)(\Gamma-1)}}{1+\frac{2y_0\delta_\kappa}{\left(u_1^s/\omega\right)^2}\frac{(1+lK_s/y_0K)(1+\epsilon_s)\left(1-\sqrt{\sigma}\right)}{(1-1/\Gamma)}}\right]
$$

Since the prandtl number (σ) for sodium (0.0049042) is very small, its square root would be larger. It is assumed that Swift discarded the σ term due to its small contribution. However, when the prandtl number for air (0.6397) is used, the additional term makes a significant difference. The difference between the two versions of the equation can be seen in Figures F.1(a) and F.1(b).
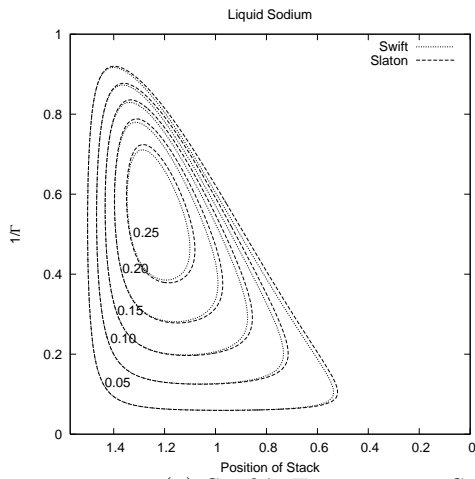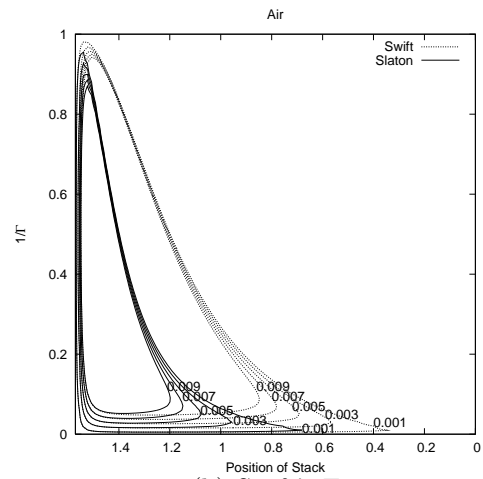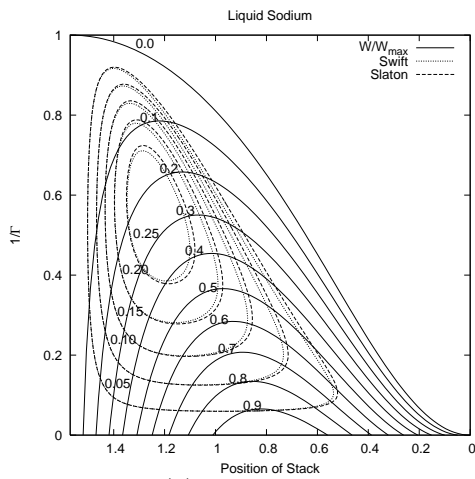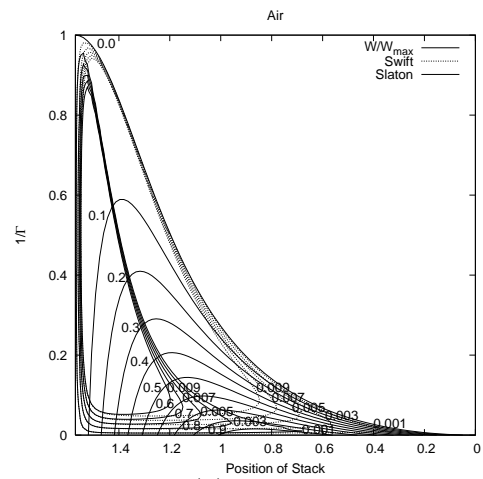
(a) Swift's Engine using Sodium
(b) Swift's Engine using Air

Figure F.1: Comparison of Swift's equation vs. Slaton's equation

(a) Swift's Engine using Sodium
(b) Swift's Engine using Air

Figure F.2: Comparison of Swift's equation vs. Slaton's equation with $\dot{W}/\dot{W}_C$

Gnuplot script file for figure F.1(a)

```
reset

pa=200*(10**5)
pm=851.975
a=2361.96

f=1000
w=2*pi*f

Ks=1.252*(10**2)
K=70.88435
```

```
dk=1.4434*(10**(-4))
Y0=1.2*dk
s=0.0049042
es=0.4
l=0.8*Y0
g=1.24

u1s(x)=pa/(pm*a)*(1+(l/Y0))*cos(x)
p1s(x)=pa*sin(x)

#SWIFT'S VERSION
F(x,y)=(2*Y0*dk)/((u1s(x)/w)**2)
G(x,y)=(1+(l*Ks)/(Y0*K))*(1+es)*(1-sqrt(s))/(1-y)
H(x,y)=1+F(x,y)*G(x,y)
A(x,y)=1+y*(1+es)*((pm*a*(u1s(x)/p1s(x)))**2)/((g-1)*(1-y))
B(x,y)=1-sqrt(s)*A(x,y)
C(x,y)=y*B(x,y)
J(x,y)=C(x,y)/H(x,y)

#SLATON'S VERSION
MM(x,y)=1-sqrt(s)*y*((pm*a*u1s(x)/p1s(x))**2)*(1+es)/((g-1)*(1-y))
NM(x,y)=y*(1-sqrt(s))*MM(x,y)
KM(x,y)=NM(x,y)/H(x,y)

set xrange[pi/2:0]
set yrange[0:1]
set size square
set view map

set isosample 100,100

set term table
set cont base
unset surface

set cntrparam levels incre 0.05,0.01,0.05
set out "CSwift05.dat"
splot J(x,y)
set out "CSlaton05.dat"
splot KM(x,y)

set cntrparam levels incre 0.10,0.01,0.10
set out "CSwift10.dat"
splot J(x,y)
set out "CSlaton10.dat"
splot KM(x,y)
```

```
set cntrparam levels incre 0.15,0.01,0.15
set out "CSwift15.dat"
splot J(x,y)
set out "CSlaton15.dat"
splot KM(x,y)

set cntrparam levels incre 0.20,0.01,0.20
set out "CSwift20.dat"
splot J(x,y)
set out "CSlaton20.dat"
splot KM(x,y)

set cntrparam levels incre 0.25,0.01,0.25
set out "CSwift25.dat"
splot J(x,y)
set out "CSlaton25.dat"
splot KM(x,y)

set label '0.05' at 1.435,0.129
set label '0.10' at 1.413,0.238
set label '0.15' at 1.385,0.310
set label '0.20' at 1.365,0.414
set label '0.25' at 1.323,0.503

set terminal postscript enhanced monochrome
set out 'swift4a.eps'

set xlabel 'Position of Stack'
set ylabel '1/{/Symbol G}'

set title 'Liquid Sodium'

plot 'CSwift05.dat' with lines lt 4 title 'Swift',\
'CSwift10.dat' with lines lt 4 notitle,\
'CSwift15.dat' with lines lt 4 notitle,\
'CSwift20.dat' with lines lt 4 notitle,\
'CSwift25.dat' with lines lt 4 notitle,\
'CSlaton05.dat' with lines lt 2 title 'Slaton',\
'CSlaton10.dat' with lines lt 2 notitle,\
'CSlaton15.dat' with lines lt 2 notitle,\
'CSlaton20.dat' with lines lt 2 notitle,\
'CSlaton25.dat' with lines lt 2 notitle
```

Gnuplot script file for figure F.2(a)

```
reset

pa=200*(10**5)
pm=851.975
a=2361.96

f=1000
w=2*pi*f

Ks=1.252*(10**2)
K=70.88435

dk=1.4434*(10**(-4))
Y0=1.2*dk
s=0.0049042
es=0.4
l=0.8*Y0
g=1.24

u1s(x)=pa/(pm*a)*(1+(l/Y0))*cos(x)
p1s(x)=pa*sin(x)

#SWIFT'S VERSION
F(x,y)=(2*Y0*dk)/((u1s(x)/w)**2)
G(x,y)=(1+(l*Ks)/(Y0*K))*(1+es)*(1-sqrt(s))/(1-y)
H(x,y)=1+F(x,y)*G(x,y)
A(x,y)=1+y*(1+es)*((pm*a*(u1s(x)/p1s(x)))**2)/((g-1)*(1-y))
B(x,y)=1-sqrt(s)*A(x,y)
C(x,y)=y*B(x,y)
J(x,y)=C(x,y)/H(x,y)

#SLATON'S VERSION
MM(x,y)=1-sqrt(s)*y*((pm*a*u1s(x)/p1s(x))**2)*(1+es)/((g-1)*(1-y))
NM(x,y)=y*(1-sqrt(s))*MM(x,y)
KM(x,y)=NM(x,y)/H(x,y)

Z1(x,R)=(g-1)*sin(x)*(sin(x)*cos(x)-R/2)
Z2(x,R)=(sin(x)**2)*cos(x)*(g-1)+sqrt(s)*(1-es)*((1+l/Y0)**2)*(cos(x)**3)
Z3(x,R)=Z1(x,R)/Z2(x,R)

set xrange[pi/2:0]
set yrange[0:1]
set size square
set view map
```

```
set isosample 100,100

set term table
set cont base
unset surface

set cntrparam levels incre 0.05,0.01,0.05
set out "CSwift05.dat"
splot J(x,y)
set out "CSlaton05.dat"
splot KM(x,y)

set cntrparam levels incre 0.10,0.01,0.10
set out "CSwift10.dat"
splot J(x,y)
set out "CSlaton10.dat"
splot KM(x,y)

set cntrparam levels incre 0.15,0.01,0.15
set out "CSwift15.dat"
splot J(x,y)
set out "CSlaton15.dat"
splot KM(x,y)

set cntrparam levels incre 0.20,0.01,0.20
set out "CSwift20.dat"
splot J(x,y)
set out "CSlaton20.dat"
splot KM(x,y)

set cntrparam levels incre 0.25,0.01,0.25
set out "CSwift25.dat"
splot J(x,y)
set out "CSlaton25.dat"
splot KM(x,y)

set label '0.0' at 1.313,0.979
set label '0.1' at 1.296,0.794
set label '0.2' at 1.219,0.666
set label '0.3' at 1.154,0.562
set label '0.4' at 1.119,0.462
set label '0.5' at 1.065,0.370
set label '0.6' at 1.022,0.290
set label '0.7' at 0.990,0.216
set label '0.8' at 0.948,0.142
```

```
set label '0.9' at 0.892,0.073

set label '0.05' at 1.435,0.129
set label '0.10' at 1.413,0.238
set label '0.15' at 1.385,0.310
set label '0.20' at 1.365,0.414
set label '0.25' at 1.323,0.503

set terminal postscript enhanced monochrome
set out 'swift4.eps'

set xlabel 'Position of Stack'
set ylabel '1/{/Symbol G}'

set title 'Liquid Sodium'

plot Z3(x,0.0) lt 1 title 'W/W_{max}',\
Z3(x,0.1) lt 1 notitle,\
Z3(x,0.2) lt 1 notitle,\
Z3(x,0.3) lt 1 notitle,\
Z3(x,0.4) lt 1 notitle,\
Z3(x,0.5) lt 1 notitle,\
Z3(x,0.6) lt 1 notitle,\
Z3(x,0.7) lt 1 notitle,\
Z3(x,0.8) lt 1 notitle,\
Z3(x,0.9) lt 1 notitle,\
'CSwift05.dat' with lines lt 4 title 'Swift',\
'CSwift10.dat' with lines lt 4 notitle,\
'CSwift15.dat' with lines lt 4 notitle,\
'CSwift20.dat' with lines lt 4 notitle,\
'CSwift25.dat' with lines lt 4 notitle,\
'CSlaton05.dat' with lines lt 2 title 'Slaton',\
'CSlaton10.dat' with lines lt 2 notitle,\
'CSlaton15.dat' with lines lt 2 notitle,\
'CSlaton20.dat' with lines lt 2 notitle,\
'CSlaton25.dat' with lines lt 2 notitle
```

Appendix G

Engine Efficiency at Maximum Power

In Schroeder's[4] discussion of heat engines and the Carnot cycle, he presents the reader a multistep problem which results in an equation for efficiency at maximum power.

To absorb heat from the the hot reservoir, the hot temperature of the working fluid (T_{hw}) must be lower than the temperature of the hot reservoir (T_h). To expel heat to the cold reservoir, the cold temperature of the working fluid (T_{cw}) must be higher than the temperature of the cold reservoir (T_c). Assuming the rate of heat transfer is proportional to the difference in temperature, we get the following two equations:

$$\frac{Q_h}{\Delta t} = k_h \left(T_h - T_{hw} \right) \tag{G.1}$$

$$\frac{Q_c}{\Delta t} = k_c (T_{cw} - T_c) \tag{G.2}$$

For the sake of simplicity, we shall assume $k_h = k_c = k$ and that Δt for both processes is the same.

Assuming that no new entropy is created during the cycle except during the two heat transfer processed, derive an equation that relates the four temperatures, T_h, T_{hw}, T_c, and T_{cw}. Dividing equation G.2 by equation G.1 yields

$$\frac{Q_c}{Q_h} = \frac{T_{cw} - T_c}{T_h - T_{hw}} \tag{G.3}$$

Power is defined as the work done over a period of time

$$P = \frac{|W|}{\Delta t_{total}} \tag{G.4}$$

Assuming Δt for the adiabatic processes are negligible,

$$\Delta t_{total} = 2\Delta t$$

Solving equation G.1 for Δt, we get

$$\Delta t = \frac{Q_h}{k \left(T_h - T_{hw} \right)}$$

substituting this value back into equation G.4 results in

$$P = \frac{|W|}{2 \left(\frac{Q_h}{k(T_h - T_{hw})} \right)} \tag{G.5}$$

from the diagram, we see that $Q_h = Q_c + W$ which can be rewritten as

$$W = Q_h - Q_c \qquad \text{(G.6)}$$

Substituting this value back into equation G.5 yields:

$$P = \frac{Q_h - Q_c}{2\left(\frac{Q_h}{k(T_h - T_{hw})}\right)}$$

which can be expressed as:

$$P = \frac{k}{2}(T_h - T_{hw})\left(1 - \frac{Q_c}{Q_h}\right) \qquad \text{(G.7)}$$

Since no new entropy is created by the engine

$$\Delta S_{hw} = \Delta S_{cw}$$

$$\frac{Q_h}{T_{hw}} = \frac{Q_c}{T_{cw}}$$

$$\frac{T_{cw}}{T_{hw}} = \frac{Q_c}{Q_h} \qquad \text{(G.8)}$$

Substituting this value back into equation G.7 yeilds

$$P = \frac{k}{2}(T_h - T_{hw})\left(1 - \frac{T_{cw}}{T_{hw}}\right) \qquad \text{(G.9)}$$

Substituting equation G.8 into equation G.3 yeilds

$$\frac{T_{cw}}{T_{hw}} = \frac{T_{cw} - T_c}{T_h - T_{hw}}$$

Solving this equation for one variable in terms of the two constants and the other variable.

$$T_{cw}T_h - T_{cw}T_{hw} = T_{cw}T_{hw} - T_cT_{hw}$$

$$2T_{cw}Thw - T_{cw}T_h = T_cT_{hw}$$

$$T_{cw} = \frac{T_cT_{hw}}{2T_{hw} - T_h} \qquad \text{(G.10)}$$

Now, we substitute this value back into equation G.9

$$P = \frac{k}{2}(T_h - T_{hw})\left(1 - \frac{\left(\frac{T_cT_{hw}}{2T_{hw} - T_h}\right)}{T_{hw}}\right)$$

$$P = \frac{k}{2}(T_h - T_{hw})\left(1 - \frac{T_c}{2T_{hw} - Th}\right)$$

To maximize the power for any fixed T_h and T_c, take the first derivative in respect to T_{hw} and solve for the zeros.

$$\frac{\mathrm{d}P}{\mathrm{d}T_{hw}} = -\frac{k}{2}\left(\frac{4T_{hw}^2 - 4T_{hw}T_h + T_h^2 - T_hT_c}{(2T_{hw} - T_h)^2}\right)$$

since only the part of the equation that is relevent is the numerator, and it is a single variable quadratic equation in T_{HW}, the use of the quadratic formula yeilds

$$T_{hw} = \frac{1}{2}\left(T_{h\,-}^{\,+}\sqrt{T_hT_c}\right)$$

if we take the limit as T_c approaches T_h we get that

$$T_{hw} = 0, T_h$$

since all temperatures are in Kelvin, 0 makes no sense as an answer, therefore

$$T_{hw} = \frac{1}{2}\left(T_h + \sqrt{T_hT_c}\right) \tag{G.11}$$

We can substitute this value back into the equation G.10, which yields

$$T_{cw} = \frac{1}{2}\left(T_c + \sqrt{T_hTc}\right) \tag{G.12}$$

Now that we have values for T_{hw} and T_{cw}, we can calculate the efficiency rating at maximum power.

$$e = \frac{benefit}{cost}$$

$$e = \frac{W}{Q_h}$$

substituting in the the heat equivalent term for work from equation G.6

$$e = \frac{Q_h - Q_c}{Q_h}$$

$$e = 1 - \frac{Q_c}{Q_h}$$

now we substitute in the entropy defined value from equation G.8

$$e = 1 - \frac{T_{cw}}{T_{hw}}$$

at this point, we substitute in the values from equations G.11 and G.12

$$e = 1 - \frac{\frac{1}{2}\left(T_c + \sqrt{T_hT_c}\right)}{\frac{1}{2}\left(T_h + \sqrt{T_hT_c}\right)}$$

which can be reduced to

$$e = 1 - \sqrt{\frac{T_c}{T_h}} \tag{G.13}$$

Let us examine a coal-fired steam engine that runs in the temperature ranges

$$T_h = 600°C = 873.15K$$

$$T_c = \quad 25°C = 298.15K$$

for these values, Carnot efficiency is

$$e = 1 - \frac{T_c}{T_h} = 1 - \frac{298.15}{873.15} = .6585$$

calculated efficiency for this engine, using equation G.13 is

$$e = 1 - \sqrt{\frac{T_c}{T_h}} = 1 - \sqrt{\frac{298.15}{873.15}} = .4157$$

if we define a new variable η as the ratio of calculated efficiency to Carnot efficiency

$$\eta = \frac{.4157}{.6585} = .6313$$

System	T_H (K)	T_C (K)	$\dot{Q}_H$ (W)	$\dot{W}$ (W)	e	η
Large TA Engine[7]	973	308	7000	630	0.09	0.13
Stirling-cycle based TA Engine[1]	998	298	5500	710	0.30	–

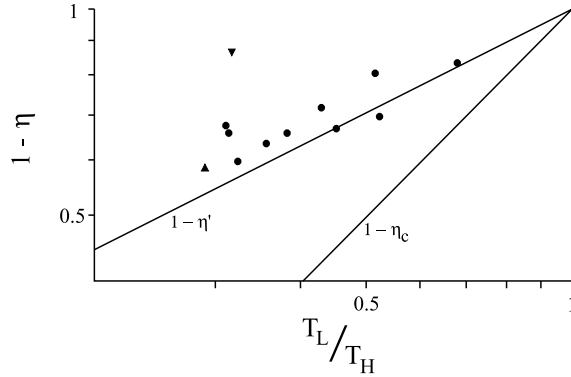Table G.1: Prime Mover data taken from published works

Figure G.1: Compilation of power-plant efficiencies. Circles represent data from Table G.2, Inverted triangle represents the large thermoacoustic engine and the upright triangle represents the Stirling-cycle based thermoacoustic engine from Table G.1

Power Plant	T_L (°C)	T_H (°C)	η_C	η'	η (observed)
West Thurrock (UK), 1962 conventional coal-fired steam plant	25	565	0.64	0.40	0.36
CANDU (Canada), PHW nuclear reactor	25	300	0.48	0.28	0.30
Larderello (Italy), geothermal steam plant	80	250	0.32	0.18	0.16
1936-1940 central steam-power stations in the UK	25	425	0.57	0.35	0.28
Calder Hall (UK), 1956 nuclear reactor	25	310	0.49	0.28	0.19
Dungeness "A" (UK), 1965 nuclear reactor	25	390	0.55	0.33	0.33
1956 steam plant in the U. S.	25	650	0.68	0.43	0.40
1949 combined-cycle (steam and mercury) plant in the U. S.	25	510	0.62	0.38	0.34
1944 closed-cycle gas turbine in Switzerland	25	690	0.69	0.44	0.38
1950 closed-cycle gas turbin in France	25	680	0.69	0.44	0.34

Table G.2: The Observed Efficiencies of Ten Power Plants[2]. Data is represented on figure G.1 by the circles

Appendix H

Refrigeration Coefficient of Performance

Working from the textbook by Bejan[2], We have the following derivations. Beginning with the basic assumption that the rate of heat flow is relative to the temperature difference, we have:

$$\dot{Q}_L = (\hbar A)_L (T_{LC} - T_L) \tag{H.1}$$
$$\dot{Q}_H = (\hbar A)_H (T_H - T_{HC}) \tag{H.2}$$

Dividing equation H.1 by equation H.2 yields the relationship:

$$\frac{\dot{Q}_L}{\dot{Q}_H} = \frac{(\hbar A)_L (T_{LC} - T_L)}{(\hbar A)_H (T_H - T_{HC})} \tag{H.3}$$

Where $(\hbar A)_x$ represents the respective heat transfer conductances. Let $(\hbar A)_H + (\hbar A)_L = (\hbar A)$.

Assuming the only entropy created in the system occurs during the heat transfers to/from the temperature reservoirs,

$$\frac{\dot{Q}_L}{T_{LC}} = \frac{\dot{Q}_H}{T_{HC}}$$

Which yields the relationship:

$$\frac{\dot{Q}_L}{\dot{Q}_H} = \frac{T_{LC}}{T_{HC}} \tag{H.4}$$

We now have two relationships for the ratio of heat transfer, equations H.3 and H.4, which we can now set equal to each other and solve for one unknown (T_{LC}) in terms of the other unknown (T_{HC}) and the two known constants $(T_H$ and $T_L)$.

$$\frac{T_{LC}}{T_{HC}} = \frac{(\hbar A)_L (T_{LC} - T_L)}{(\hbar A)_H (T_H - T_{HC})}$$
$$T_{LC} = \frac{(\hbar A)_L T_L T_{HC}}{(\hbar A)_L T_{HC} - \dot{Q}_H}$$
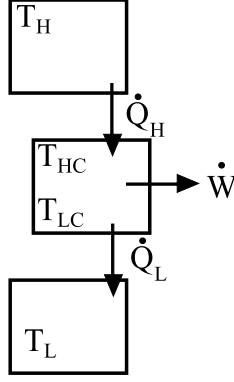$$T_{LC} = \frac{T_L T_{HC}}{T_{HC} - \frac{\dot{Q}_H}{(\hbar A)_L}} \tag{H.5}$$

Figure H.1:

Looking at figure H.1 we can define work, do some simple manipulation of the equation and then substitute in the results of equations H.3 and H.5.

$$
\begin{aligned}
\dot{W} &= \dot{Q}_{HC} - Q_{LC} \\
&= \dot{Q}_{HC}\left(1 - \frac{\dot{Q}_{LC}}{\dot{Q}_{HC}}\right) \\
&= \dot{Q}_{HC}\left(1 - \frac{T_{LC}}{T_{HC}}\right) \\
&= \dot{Q}_{H}\left(1 - \frac{T_L}{T_{HC} - \frac{\dot{Q}_H}{(\hbar A)_L}}\right)
\end{aligned}
\tag{H.6}
$$

Now we have all the pieces we need to calculate efficiency (η).

$$
\begin{aligned}
\eta &= \frac{\text{benefit}}{\text{cost}} \\
&= \frac{\dot{W}}{\dot{Q}_H} \\
&= \frac{\dot{Q}_H\left(1 - \frac{T_L}{T_{HC} - \frac{\dot{Q}_H}{(\hbar A)_L}}\right)}{\dot{Q}_H} \\
&= \left(1 - \frac{T_L}{T_{HC} - \frac{\dot{Q}_H}{(\hbar A)_L}}\right)
\end{aligned}
\tag{H.7}
$$

Going back to equation H.2, we can rearrange it for T_{HC}.

$$
\begin{aligned}
\dot{Q}_H &= (\hbar a)_H\,(T_H - T_{HC}) \\
\frac{\dot{Q}_H}{(\hbar a)_H} &= T_H - T_{HC} \\
T_{HC} &= T_H - \frac{\dot{Q}_H}{(\hbar a)_H}
\end{aligned}
\tag{H.8}
$$

Substituting equation H.8 into equation H.7 we get

$$
\begin{aligned}
\eta &= 1 - \frac{T_L}{T_H - \frac{\dot{Q}_H}{(\hbar A)_H} - \frac{\dot{Q}_H}{(\hbar A)_l}} \\
&= 1 - \frac{T_L}{T_H - \dot{Q}_H \left(\frac{1}{(\hbar A)_H} + \frac{1}{(\hbar A)_L} \right)}
\end{aligned}
\tag{H.9}
$$

Returning to the relationship $(\hbar A)_H + (\hbar A)_L = (\hbar A)$, we can write $(\hbar A)_H$ as $x\hbar A$ and $(\hbar A)_L$ as $(1-x)\hbar A$. Substituting these into equation H.9 we get

$$
\begin{aligned}
\eta &= 1 - \frac{T_L}{T_H - \dot{Q}_H \left(\frac{1}{x\hbar A} + \frac{1}{(1-x)\hbar A} \right)} \\
&= 1 - \frac{T_L}{T_H - \frac{\dot{Q}_H}{\hbar A} \left(\frac{1}{x} + \frac{1}{(1-x)} \right)} \\
&= 1 - \frac{\frac{T_L}{T_H}}{1 - \frac{\dot{Q}_H}{T_H \hbar A} \left(\frac{1}{x} + \frac{1}{1-x} \right)}
\end{aligned}
\tag{H.10}
$$

By taking the first derivative of equation H.10 in respect to x and setting equal to 0, we find the x value when η is at its maximum. This gives us $x = \frac{1}{2}$. Putting this back into equation H.10 we get

$$
\begin{aligned}
\eta_{\text{max}} &= 1 - \frac{\frac{T_L}{T_H}}{1 - \frac{\dot{Q}_H}{T_H \hbar A} \left(\frac{1}{\frac{1}{2}} + \frac{1}{1-\frac{1}{2}} \right)} \\
&= 1 - \frac{\frac{T_L}{T_H}}{1 - \frac{4\dot{Q}_H}{T_H \hbar A}}
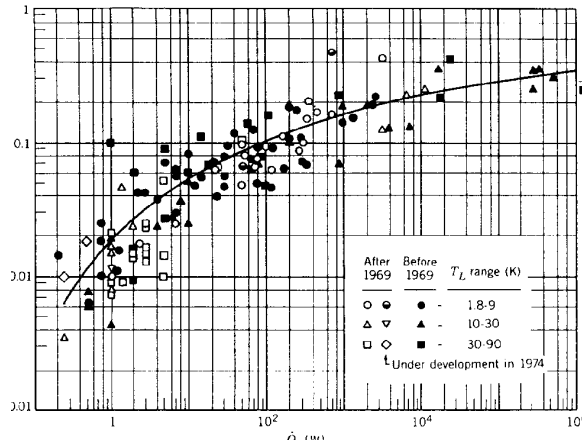\end{aligned}
\tag{H.11}
$$

Figure H.2: Compilation of second-law efficiencies of refrigerators and liquefiers[2]. The horizontal axis is $\dot{Q}_L$ measured in watts (W) and the vertical axis is η_{II}.

Circles		Triangles		Squares	
$\dot{Q}_L(W)$	η_{II}	$\dot{Q}_L$ (W)	η_{II}	$\dot{Q}_L$ (W)	η_{II}
115.0982	0.04657379	193.5563	0.1001852	93.18556	0.048019309
115.0982	0.06.2583543	864.7740	0.069309466	103.5919	0.1614227
119.2164	0.09.3116477	961.1516	0.1861852	876.0496	0.2282480
169.4368	0.06.4525962	3127.665	0.1237050	17900.84	0.2169118
160.7337	0.1130049	3863.654	0.1275147	23739.90	0.4249311
195.0187	0.1084921	7031.318	0.1300535		
287.0882	0.072917514	6438.663	0.2231915		
324.6761	0.069295965	11114.49	0.2469808		
262.9344	0.087594710	16664.69	0.3490688		
292.1789	0.1010240				
277.1712	0.1096031				
330.4334	0.1518504				
445.5074	0.1698590				
348.3251	0.2061386				
691.3447	0.1630757				
679.2991	0.4801931				
948.6353	0.1428457				
1301.679	0.1549764				
2324.943	0.1939146				
2538.518	0.2236441				
3079.992	0.4336787				

Table H.1: Data extracted from figure H.2 using xyExtract.

System	T_0 (K)	T_C (K)	$\dot{Q}_L$ (W)	$\dot{W}$ (W)	COP	COPR	C_i^*
Tijani [11]	288	243	4	–	–	0.115	–
Swift [9]	300	133	7000	30000		0.25#	
Poese-Garrett [3]	300	290	30.77*	50.04*	–	–	–

Table H.2: Refrigerator data taken from other published works.
Values marked with * are extracted from graphs using xyExtract.
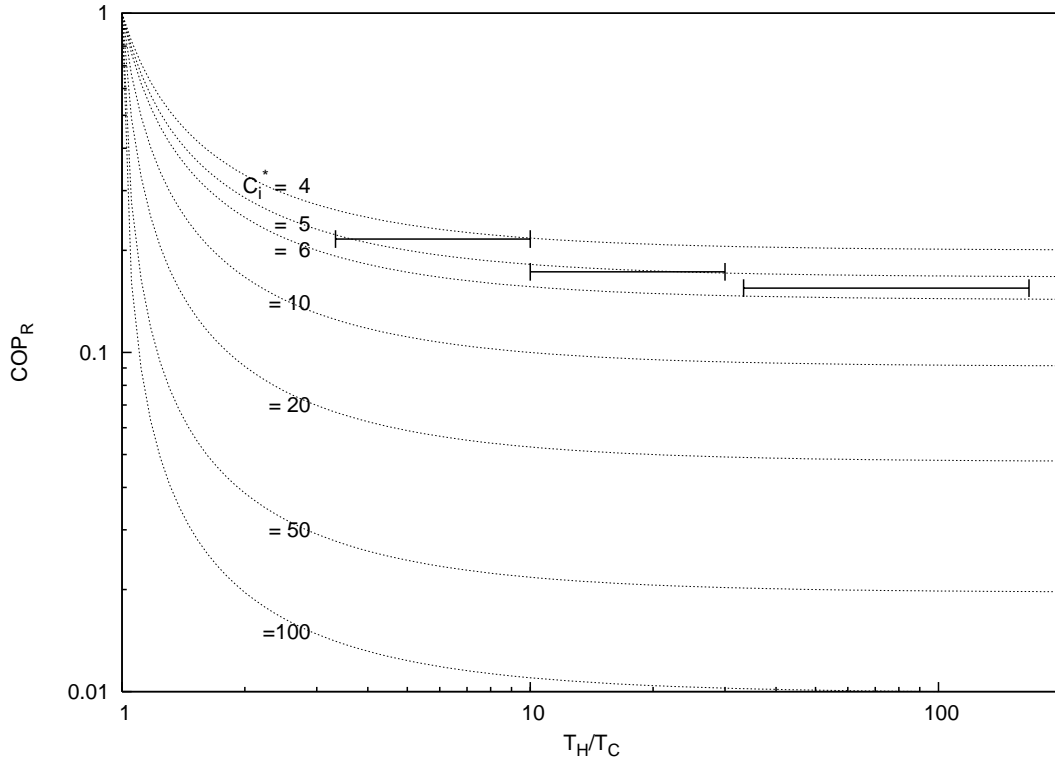Values marked with # are calculated from values in this table

Figure H.3: Enhanced Reproduction of graph from Bejan's[2] text. The constant C_i^* is the internal conductance of the system. The horizontal bars represent Empirical data.
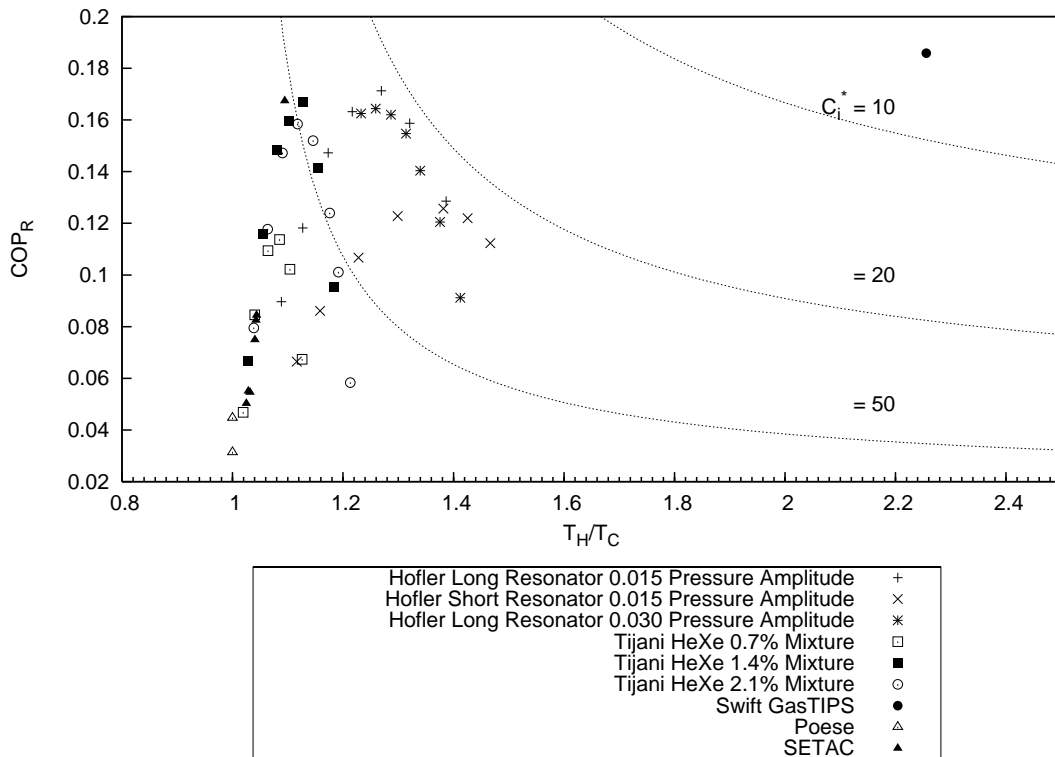

Figure H.4: Thermoacoustic system data plotted against graph similar to Figure H.3

45

Bibliography

[1] S. Backhaus and G. W. Swift. A thermoacoustic-stirling heat engine: Detailed study. *Journal of the Acoustical Society of America*, 107(6):3148–3166, Jun 2000.

[2] Adrian Bejan. *Advanced Engineering Thermodynamics, Second Edition.* John Wiley & Sons, Inc., 1997.

[3] Matthew E. Poese and Steven L. Garrett. Performance measurements on a thermoacoustic refrigerator driven at high amplitudes. *Journal of the Acoustical Society of America*, 107(5):2480–2486, May 2000.

[4] Daniel V. Schroeder. *An Introduction to Thermal Physics.* Addison Wesley Longman, 2000.

[5] Raymond A. Serway. *Physics For Scientiest & Engineers with Modern Physics.* Saunders College Publishing, 1982.

[6] G. W. Swift. Thermoacoustic engines. *Journal of the Acoustical Society of America*, 84(4):1145–1180, 1988.

[7] G. W. Swift. Analysis and performance of a large thermoacoustic engine. *Journal of the Acoustical Society of America*, 92(3):1151–1563, Sep 1992.

[8] G. W. Swift. *Thermoacoustice: A unifying perspective for some engines and refrigerators.* Acoustical Society of America, 2002.

[9] Greg Swift and John Wollan. Thermoacoustics for liquification of natural gas. *GasTIPS*, Fall, 2002.

[10] Gregory W. Swift. Thermoacoutic engines and refrigerators. *Physics Today*, 48, 1995.

[11] Moulay El Hassan Tijani. *Loudspeaker-driven thermo-acoustic refrigeration.* PhD thesis, Technische Universiteit Eindhoven, 2001.

[12] Henry E. Bass W. Pat Arnott and Richard Raspet. General formulation of thermoacoustics for stacks having arbitrarily shaped pore cross sections. *Journal of the Acoustical Society of America*, 90(6):3228–3237, Dec 1991.